Available online at www.sciencedirect.com
SCIENCE DIRECT®
Geochimica et Cosmochimica Acta 70 (2006) 2454–2479
Geochimica
www.elsevier.com/locate/gca

Paleowaters in Silurian-Devonian carbonate aquifers: Geochemical evolution of groundwater in the Great Lakes region since the Late Pleistocene

J.C. McIntosh [a,*], L.M. Walter [b]

[a] *Morton K. Blaustein Department of Earth and Planetary Sciences, Johns Hopkins University, Baltimore, MD 21218, USA*
[b] *Department of Geological Sciences, University of Michigan, Ann Arbor, MI 48109, USA*

Received 15 August 2005; accepted in revised form 1 February 2006

Abstract

Changes in the climatic conditions during the Late Quaternary and Holocene greatly impacted the hydrology and geochemical evolution of groundwaters in the Great Lakes region. Increased hydraulic gradients from melting of kilometer-thick Pleistocene ice sheets reorganized regional-scale groundwater flow in Paleozoic aquifers in underlying intracratonic basins. Here, we present new elemental and isotopic analyses of 134 groundwaters from Silurian-Devonian carbonate and overlying glacial drift aquifers, along the margins of the Illinois and Michigan basins, to evaluate the paleohydrology, age distribution, and geochemical evolution of confined aquifer systems. This study significantly extends the spatial coverage of previously published groundwaters in carbonate and drift aquifers across the Midcontinent region, and extends into deeper portions of the Illinois and Michigan basins, focused on the freshwater–saline water mixing zones. In addition, the hydrogeochemical data from Silurian-Devonian aquifers were integrated with deeper basinal fluids, and brines in Upper Devonian black shales and underlying Cambrian-Ordovician aquifers to reveal a regionally extensive recharge system of Pleistocene-age waters in glaciated sedimentary basins. Elemental and isotope geochemistry of confined groundwaters in Silurian-Devonian carbonate and glacial drift aquifers show that they have been extensively altered by incongruent dissolution of carbonate minerals, dissolution of halite and anhydrite, cation exchange, microbial processes, and mixing with basinal brines. Carbon isotope values of dissolved inorganic carbon (DIC) range from −10 to −2‰, $^{87}Sr/^{86}Sr$ ratios range from 0.7080 to 0.7090, and $\delta^{34}S$–SO_4 values range from +10 to 30‰. A few waters have elevated $\delta^{13}C_{DIC}$ values (>15‰) from microbial methanogenesis in adjacent organic-rich Upper Devonian shales. Radiocarbon ages and $\delta^{18}O$ and δD values of confined groundwaters indicate they originated as subglacial recharge beneath the Laurentide Ice Sheet (14–50 ka BP, −15 to −13‰ $\delta^{18}O$). These paleowaters are isolated from shallow flow systems in overlying glacial drift aquifers by lake-bed clays and/or shales. The presence of isotopically depleted waters in Paleozoic aquifers at relatively shallow depths illustrates the importance of continental glaciation on regional-scale groundwater flow. Modern groundwater flow in the Great Lakes region is primarily restricted to shallow unconfined glacial drift aquifers. Recharge waters in Silurian-Devonian and unconfined drift aquifers have $\delta^{18}O$ values within the range of Holocene precipitation: −11 to −8‰ and −7 to −4.5‰ for northern Michigan and northern Indiana/Ohio, respectively. Carbon and Sr isotope systematics indicate shallow groundwaters evolved through congruent dissolution of carbonate minerals under open and closed system conditions ($\delta^{13}C_{DIC} = -14.7$ to −11.1‰ and $^{87}Sr/^{86}Sr = 0.7080$–0.7103). The distinct elemental and isotope geochemistry of Pleistocene- versus Holocene-age waters further confirms that surficial flow systems are out of contact with the deeper basinal-scale flow systems. These results provide improved understanding of the effects of past climate change on groundwater flow and geochemical processes, which are important for determining the sustainability of present-day water resources and stability of saline fluids in sedimentary basins.

* Corresponding author. Fax: +1 410 516 7933.
E-mail address: jmcintosh@jhu.edu (J.C. McIntosh).

0016-7037/$ - see front matter © 2006 Elsevier Inc. All rights reserved.
doi:10.1016/j.gca.2006.02.002

1. Introduction

The low-lying interior of North America is characterized by a number of intracratonic sedimentary basins (Fig. 1). These relatively undeformed depressions contain Paleozoic to Mesozoic-age strata and highly saline formation waters, and are overlain by a thin layer of quaternary sediments and dilute meteoric waters. The basin hydrostratigraphic units are compartmentalized into regional aquifer systems and confining units that are continuous between the Illinois, Michigan and Appalachian basins (Fig. 2a). Advance and retreat of kilometer-thick ice sheets, most recently during the Late Pleistocene, exposed the Silurian-Devonian and Cambrian-Ordovician regional aquifer systems along the margins of the three basins and recharged large volumes of glacial meltwaters to great depths, profoundly altering basinal-scale groundwater flow and salinity gradients (Siegel and Mandle, 1984; McIntosh et al., 2002). Recharge of meteoric waters into the Silurian-Devonian carbonate aquifers migrated into overlying fractured, organic-rich Upper Devonian shales enhancing generation of economic reservoirs of microbial gas (methane).

This study presents new elemental and isotopic analyses of groundwaters in Silurian-Devonian carbonate and overlying glacial drift aquifers along the margins of the Illinois and Michigan basins, integrated with previously published groundwaters and basinal formation waters (Stueber and Walter, 1991; Wilson and Long, 1993a,b; Nicholas et al., 1996; Eberts and George, 2000; Ku, 2001; Lyons et al., 2002; McIntosh et al., 2002). This regionally expansive geochemical database is used to evaluate the impact of Pleistocene glaciation on regional-scale flow patterns and the geochemical evolution of paleowaters within confined aquifer systems. Understanding the paleohydrology of regional aquifers has important implications for the residence times and sustainability of drinking water resources, migration of the freshwater–saline water interface, and climate change perturbations to groundwater flow systems.

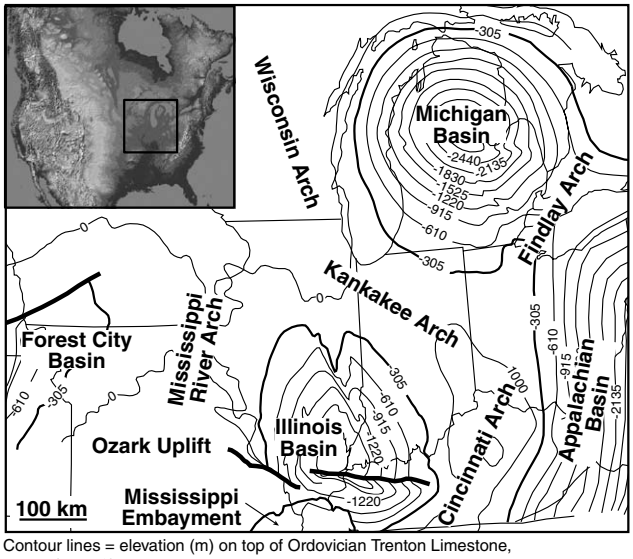

Fig. 1. Structural geology and topographic relief of the stable interior of the North American craton, modified from Collinson et al. (1988).

The hydrology and geochemistry of the Cambrian-Ordovician aquifer system has been extensively studied, motivated by large-scale groundwater withdrawal of the aquifer supplying the densely populated Chicago area. Multiple studies, including a Regional Aquifer-System Analysis (RASA) study by the US Geological Survey (Siegel, 1989), have shown that Pleistocene-age waters invaded the Cambrian-Ordovician aquifers along the margins of the Illinois and adjacent Forest City basins (Bond, 1972; Siegel and Mandle, 1984; Siegel, 1990, 1991). Isotopically depleted glacial meltwaters migrated to great depths within the Illinois Basin, mixing with saline formation waters (Stueber and Walter, 1994). Ice-induced hydraulic loading also likely impacted the Cambrian-Ordovician aquifers in the Michigan Basin, as shown by anomalous fluid pressures in the deep basin sections (Bahr et al., 1994). The Maquoketa Shale confines the Cambrian-Ordovician aquifer system, separating it from the overlying Silurian-Devonian carbonate aquifers.

A similar RASA study was conducted on the hydrogeochemistry of the Silurian-Devonian aquifer system in the arches region between the Illinois, Michigan, and Appalachian basins (Eberts and George, 2000), focusing on drinking water resources in the recharge areas of the Silurian-Devonian carbonate subcrop. Results obtained for a limited number of groundwater samples confined beneath lake-bed clays near Lake Erie had $\delta^{18}O$ and δD values consistent with recharge under cooler climatic conditions. Additional water-quality data from Silurian-Devonian carbonate aquifers, along the southeastern margin of the Michigan Basin, were also published by the US Geological Survey (Nicholas et al., 1996). Weaver et al. (1995) show that the Lower Devonian Dundee formation in southwestern Ontario (eastern Michigan Basin) was diluted by meteoric water, likely during the Pleistocene. The few studies that have been done on the expansive Silurian-Devonian carbonate aquifer system along the northern margin of the Michigan Basin have focused on shallow groundwater–surface water interactions and carbon transport at the watershed-scale (Ku, 2001; Williams, 2005). Other units, such as the Mississippian-Pennsylvanian aquifers in the Illinois and Michigan basins, have also been influenced by Pleistocene meteoric water invasion (Long et al., 1988; Ging et al., 1996; Meissner et al., 1996; Hoaglund et al., 2004; Ma et al., 2004).

This study significantly extends the well coverage of previously published groundwaters in Silurian-Devonian carbonate and glacial drift aquifers across the Midcontinent region, and into deeper portions of the Illinois and Michigan basins, focusing on the freshwater–saline water mixing zones. In addition, the hydrogeochemistry of Silurian-Devonian groundwaters is integrated with deeper basinal fluids, and brines in overlying Upper Devonian black shales and underlying Cambrian-Ordovician aquifers to reveal a

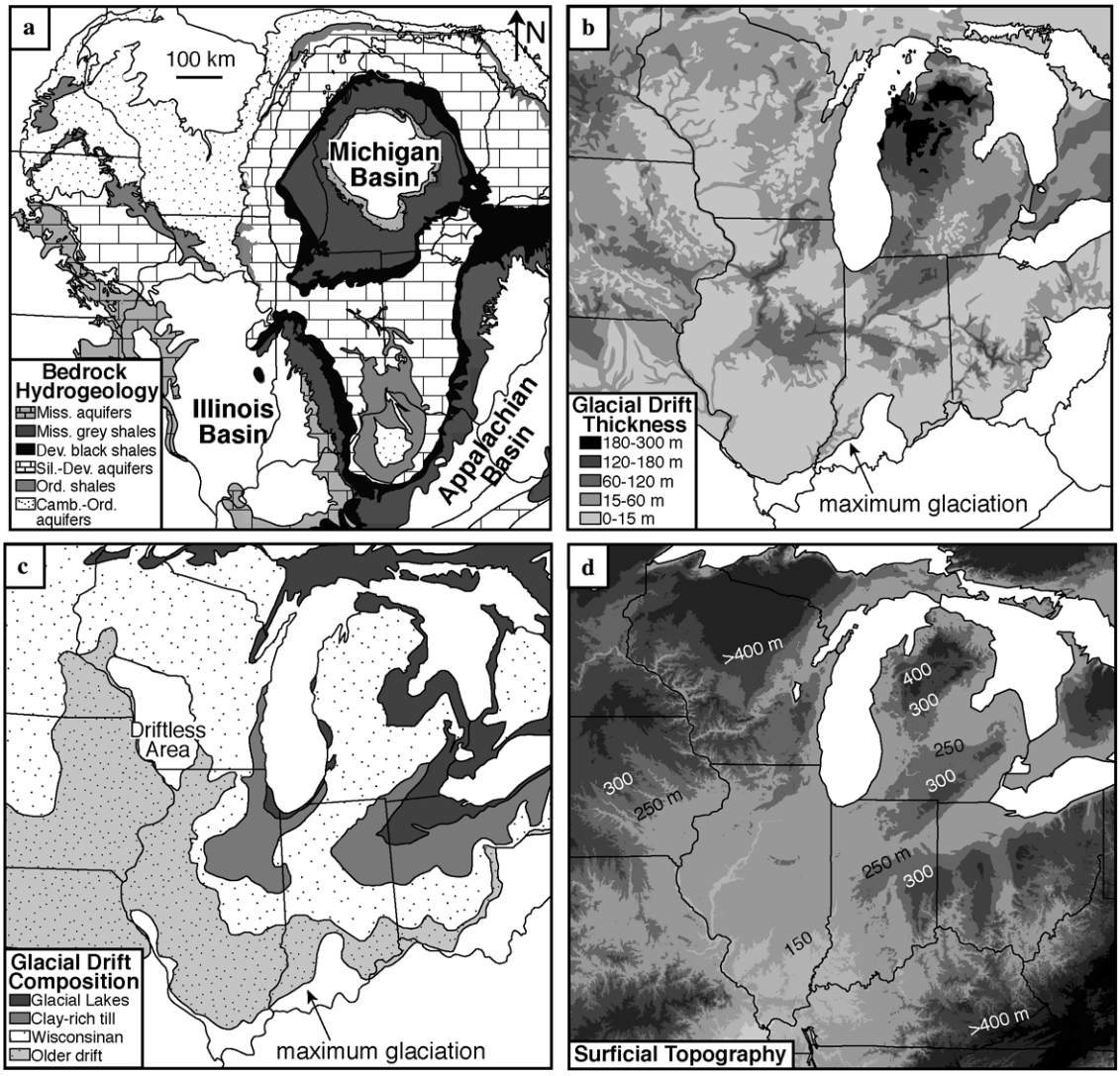

Fig. 2. Hydrogeologic framework of the Midcontinent region of the United States. (a) Geologic map of Paleozoic regional aquifers and confining units along the margins of the Illinois, Michigan, and Appalachian sedimentary basins. (b) Thickness of overlying Pleistocene glacial drift deposits, adapted from Olcott (1992), and Lloyd and Lyke (1995). (c) Lithology of surficial deposits, modified from Krothe and Kempton (1988). (d) Surficial topography.

regionally extensive recharge system of Pleistocene-age waters in intracratonic sedimentary basins.

2. Hydrogeology

The hydrogeology of the Great Lakes region is summarized in Fig. 2. The Silurian-Devonian and Cambrian-Ordovician aquifer systems subcrop along the margins of the Illinois, Michigan, and Appalachian basins (Fig. 2a). The basal Cambrian-Ordovician aquifers in all three basins are principally comprised of sandstones and carbonates (dolomite and limestone), confined by the overlying Maquoketa grey shale (also referred to as the Utica Shale). The Silurian carbonates in the Michigan and Appalachian basins contain thick sequences (~1 km) of bedded halite and anhydrite, predominately in the Salina Group, which are relatively impermeable (Vugrinovich, 1988). Overlying Devonian carbonates also contain localized halite and anhydrite. Deposition of relatively impermeable lake-bed clays and tills during the Pleistocene helped to preserve the highly soluble evaporite minerals at shallow depths along the basin margins. Extensive evaporite deposits are absent in the Illinois Basin. Silurian-Devonian aquifers are primarily composed of dolomite and limestone (Dorr and Eschman, 1970; Shaver et al., 1970). The carbonate aquifers are confined by the overlying Upper Devonian black shales, and Mississippian grey shales and siltstones. These confining units separate the Silurian-Devonian aquifer system from the overlying Mississippian clastic and carbonate aquifer system.

Continental glaciation unroofed Paleozoic aquifers along the underlying basin margins, carved out the Great Lakes basins, and deposited Pleistocene sediments of varying thickness and permeability (Figs. 2b and c). The Laurentide Ice Sheet covered the state of Michigan, northern Indiana and Ohio, during the Last Glacial Maximum

(18,000 years BP). By 14,000 years BP, the ice sheet had rapidly retreated to mid-Michigan, and by 12,600 years BP the ice sheet covered only the northern lower peninsula of Michigan. Large proglacial lakes formed in front of the retreating ice sheet (Fig. 2c). By 11,000 years BP, the ice sheet had receded to north of Lake Superior. The Great Lakes are relatively young geologic features, formed less than ~14,000 years BP, and are shallow compared to the deeper structure of the underlying basins. Glacial meltwaters likely penetrated into the regional aquifer systems during basal melting of the kilometer-thick ice sheets and lake-level fluctuations (Siegel and Mandle, 1984; Breemer et al., 2002; Hoaglund et al., 2004).

Most of the topographic relief in this relatively low-lying region is related to the thickness of glacial drift deposits (Figs. 2b–d). Modern groundwater flows from topographic highs (recharge areas) composed of permeable glacial till and outwash, to low-lying lakes and streams (discharge areas) underlain by relatively impermeable clays. The vast majority of groundwaters discharge into the Great Lakes catchment, with less than 2% of meteoric water discharging into the deeper basinal-scale flow system (Eberts and George, 2000). During Pleistocene glaciation, the regional groundwater flow patterns were reorganized by increased hydraulic gradients from melting of the ice sheets. Meteoric waters discharged into the structural Illinois and Michigan basins along the dip of the Silurian-Devonian and Cambrian-Ordovician aquifers, migrating hundreds of meters from the basin margins and significantly suppressing the fluid salinity (Siegel and Mandle, 1984; McIntosh et al., 2002). Glacial meltwater recharge into Silurian-Devonian aquifers was economically significant as dilute waters migrated into fractured Upper Devonian black shales and generated geologically recent deposits of natural gas at relatively shallow depths, along the basin margins.

3. Methods

One hundred and thirty-four groundwater samples were collected from household wells screened in Devonian carbonate bedrock and overlying glacial drift aquifers, along the margins of the Michigan and Illinois basins (Fig. 3). Well locations were chosen to achieve a diverse spatial sampling both with depth and laterally across the Devonian carbonate subcrop. In addition, samples were collected along several transects into the Michigan and Illinois basins. Detailed well location information, field parameters, and elemental and isotope analyses of groundwaters are provided in Tables 1 and 2.

Groundwater samples were collected from outside taps in a HDPE bucket, once temperature and dissolved O_2 levels had stabilized under laminar flow conditions. The pH was measured immediately, using a Corning 315 high sensitivity pH meter and an Orion Ross Combination electrode. Fluid samples were then filtered with a 0.45 μM nylon filter, before being preserved for geochemical analyses. Samples for alkalinity, cation, and anion analyses were kept in HDPE bottles with no headspace, and samples for cation analyses were acidified to pH <2 with nitric acid. Samples for dissolved inorganic carbon (DIC) and carbon isotope analyses were preserved with $CuCl_2$ to prevent biodegradation and kept in capped glass serum vials with no headspace. Dissolved organic carbon (DOC) sample aliquots were acidified with HCl and kept in glass scintillation vials. Samples for oxygen and hydrogen isotope analyses were also sealed in glass scintillation vials. All samples were kept on ice in the field and refrigerated in the laboratory prior to analysis. Unfiltered samples were collected for tritium and ^{14}C, in 500 mL HDPE and borosilicate glass bottles, respectively, with no headspace. Carbon-14 samples were then preserved with $HgCl_2$ following the methods of Castro et al. (2000).

Alkalinity was measured by the Gran-alkalinity titration method described in Gieskes and Rogers (1973) (precision, ±0.6%), within 24 h of sample collection. For these groundwaters, which lack appreciable organic acid anions or hydrogen sulfide, titration alkalinity is equal to carbonate alkalinity ($[HCO_3^-] + 2[CO_3^{2-}]$). The DIC ($[H_2CO_3] + [HCO_3^-] + [CO_3^{2-}]$) concentrations were measured by using an UIC 5011 carbon coulometer (precision, ±2%). The DOC content was measured by combustion and infrared detection of CO_2 on a Shimadzu TOC-5000A (uncertainty, ±0.1 mM).

Cation chemistry was determined by inductively coupled plasma-atomic emission spectrometry with a Leeman Labs PlasmaSpec III system, with a precision of ±2% for major elements and ±5% for minor elements. Anions were analyzed by ion chromatography (IC) with a Dionex 4000I series and AS14 column (precision, ±1%). Charge balance calculations were always within 5%.

Stable isotope chemistry (O, H, and C) was analyzed in the Stable Isotope Geochemistry Laboratory at the University of Michigan and the Environmental Isotope Geochemistry Laboratory at the University of Waterloo. Oxygen isotope ratios were determined by the CO_2 equilibration method using a modified version of the method described in Socki et al. (1992) (precision, ±0.1‰). Hydrogen isotope ratios were determined by a Zn-reduction method described by Venneman and O'Neil (1993) (precision, ±2‰). Both oxygen and hydrogen isotope ratios were measured on a Finnegan MAT-Delta S mass spectrometer. Isotope ratios are expressed in standard δ notation relative to Vienna standard mean ocean water (VSMOW). Aliquots for carbon isotope composition of DIC were prepared by off-line CO_2 extraction using a N_2-purged syringe and subsequent addition of phosphoric acid in vacuo. Carbon isotope ratios were measured on a Finnegan MAT-Delta S mass spectrometer (precision, ±0.1‰), and ratios are expressed in standard δ notation relative to Vienna Peedee Belemnite (VPDB).

Strontium, from acidified ICP aliquots, was separated by ion exchange chromatography, using ion specific resin, and $^{87}Sr/^{86}Sr$ ratios were measured by thermal ionization mass spectrometry, in the Radiogenic Isotope Geochemistry Laboratory at the University of Michigan, following standard procedures (Blum et al., 1998). The strontium concentration and isotopic composition of the nitric acid used to acidify the ICP samples was also measured and determined to not have significantly altered the strontium isotope ratios of the samples. The $^{87}Sr/^{86}Sr$ ratios were normalized for mass fractionation to $^{87}Sr/^{86}Sr = 0.1194$. Analyses of SRM-987 yielded a mean $^{87}Sr/^{86}Sr$ ratio of 0.710243 ± 11 ($\pm 2\sigma$, $n = 3$) during the period of analyses.

Sulfur and oxygen isotope ratios of SO_4^{2-} were measured on IC sample aliquots at the University of Waterloo. Sulfate in the samples was recovered as $BaSO_4$ for analysis of $\delta^{34}S$– and $\delta^{18}O$–SO_4^{2-}. Sulfur isotope ratios are reported in standard δ notation relative to Canyon Diablo Triolite (CDT) (precision = < ± 0.56), and $\delta^{18}O$ values of SO_4^{2-} are reported in standard δ notation relative to VSMOW (precision = < ± 0.68). The low SO_4^{2-} concentration (<0.42 mM) and limited sample size of many of the groundwater samples, especially in northwestern Ohio, prevented analysis of oxygen and sulfur isotopes of SO_4^{2-}. Tritium and carbon-14 were also analyzed at the University of Waterloo. Enriched tritium was measured by liquid scintillation counting (precision shown in Table 2), following the methods of Drimmie et al. (1993) and Taylor (1977), and the ^{14}C activity of the DIC was then determined on samples with no detectable tritium, by beta liquid scintillation counting (precision = ±0.18%).

Aqueous species distribution and mineral saturation state modeling were performed, using SolminEQ.88 (Kharaka et al., 1988). Log PCO_2 and saturation indices for calcite and gypsum are reported in Table 2, calculated from SolminEQ.88. The saturation state (Log IAP/K) for dolomite was calculated, using the K equilibrium value for moderately ordered sedimentary dolomite from Hyeong and Capuano (2001). To compare the ion activity product for dolomite ($CaMg(CO_3)_2$) on the

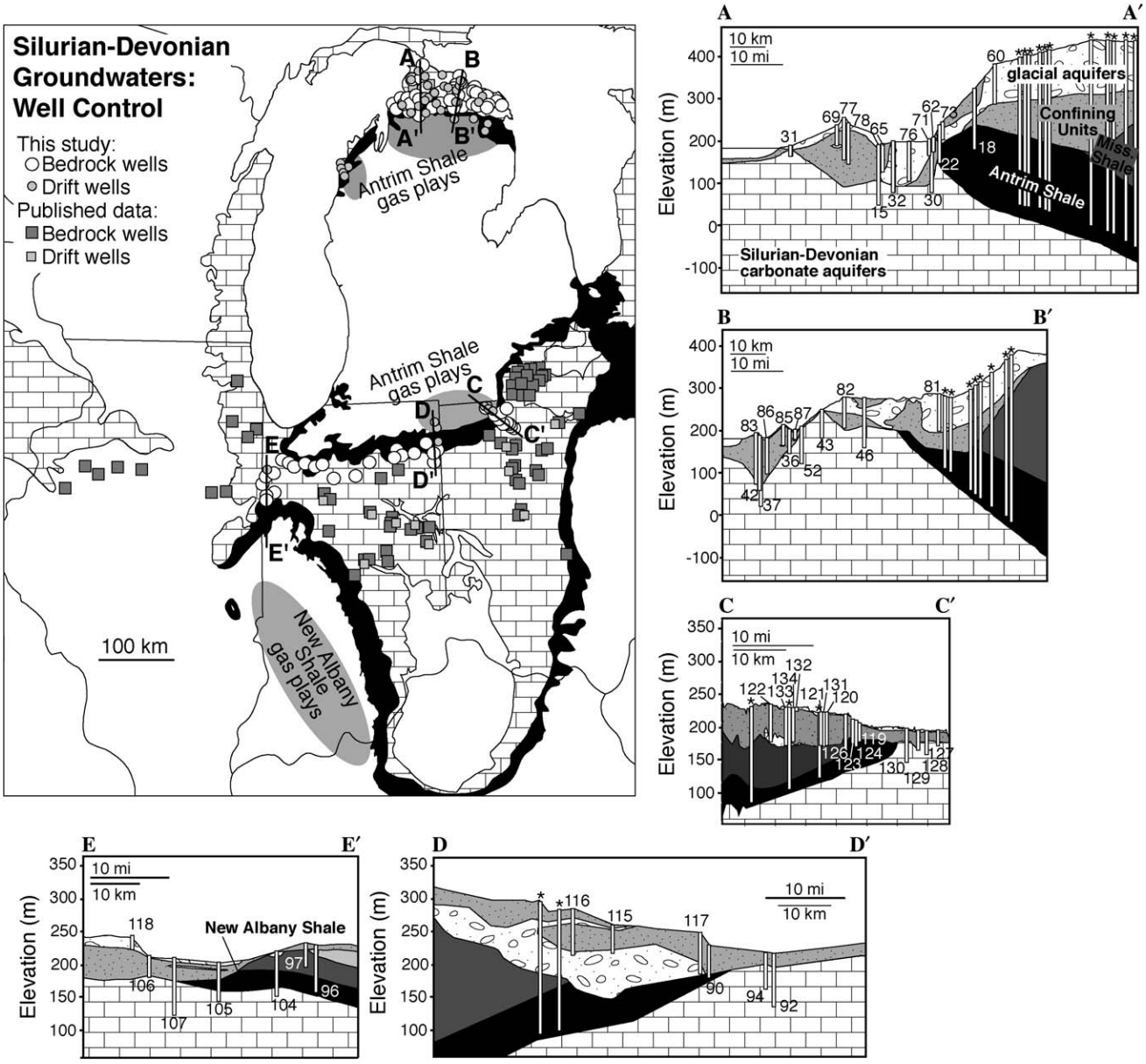

Fig. 3. Spatial and depth relations of groundwater wells in Silurian-Devonian carbonate and glacial drift aquifers. The location map displays the well control for this study relative to the Silurian-Devonian carbonate subcrop and adjacent Upper Devonian black shales. The circles represent wells sampled as part of this study, and grey squares represent previously published data (Eberts and George, 2000; Ku, 2001; Nicholas et al., 1996). Economic deposits of microbial gas (fields highlighted in grey) are located predominately in areas inundated by meteoric water recharge through the Silurian-Devonian carbonate aquifers. Geologic cross-sections were constructed along several transects into the Michigan and Illinois basins where groundwaters were collected, to constrain the hydrogeology, groundwater flow paths, and bedrock and glacial drift composition. Well ID numbers are shown above the glacial drift wells and below the bedrock wells, corresponding with fluid chemistry in Tables 1–4. Microbial gas wells are indicated by asterisk symbols. Note the differences in scale between the cross-sections.

same molar basis as calcite ($CaCO_3$), the square root was taken of the ion activity product (IAP dolomite) from SolminEQ.88. The computer program NETPATH (Plummer et al., 1994) was used to develop mass-balance models of the changes in chemical composition of groundwaters along flow paths, from recharge areas (initial well) downgradient to discharge areas (final well) (Table 3). The number of potential models was constrained by the mineralogy of the aquifers, mineral saturation states, and elemental and isotope geochemistry. NETPATH, in addition to several other mixing and mass-balance models, was also used to estimate the radiocarbon ages of groundwaters (Table 4). These carbon-14 models are discussed in greater detail in the Section 4.

Additional elemental and isotope geochemical data from the following published sources were integrated with this new dataset: Meents et al. (1952); Keller (1983); Stueber and Walter (1991); Wilson and Long (1993a,b); Weaver et al. (1995); Nicholas et al. (1996); Eberts and George (2000); Ku (2001); Lyons et al. (2002); and McIntosh et al. (2002). Sample locations of these published datasets are shown in Fig. 3.

Detailed geologic cross-sections were constructed along several transects into the Michigan and Illinois basins (Fig. 3), where groundwater samples were collected, to constrain the hydrogeology, groundwater flow paths, and bedrock and glacial drift composition. Depth and stratigraphic information were obtained from oil and gas, and groundwater well logs, and were combined with topographic and bedrock geology maps.

Table 1
Well location, carbon parameters, and major ion chemistry of groundwaters in bedrock and glacial drift aquifers

Date	ID#	County	Latitude	Longitude	Depth (m)	pH	T (°C)	Alkalinity (meq/kg)	DIC (mmol/kg)	DOC (mM)	Na (mM)	Ca (mM)	Mg (mM)	K (μM)	Sr (μM)	Cl (mM)	SO_4 (mM)
Michigan bedrock wells																	
6/20/01	1	Charlevoix	45.28298	−85.24454	96	7.59	9.4	4.09	3.67	0.13	0.289	1.195	0.856	34.53	17.12	0.046	0.125
6/20/01	2	Charlevoix	45.22662	−85.00890	86	8.52	10.7	3.36	3.06	0.18	2.479	0.324	0.252	26.60	2.56	0.095	0.055
6/20/01	3	Charlevoix	45.27615	−85.07237	59	7.54	10	4.07	4.03	0.12	0.109	1.702	0.597	21.38	0.38	0.105	0.214
6/20/01	4	Charlevoix	45.18143	−84.87417	107	9.21	10.5	4.51	3.64	0.05	4.524	0.037	0.021	7.29	0.16	0.093	0.059
6/20/01	5	Charlevoix	45.35588	−85.15511	19	7.47	9.9	5.14		0.11	0.192	1.719	0.983	20.23	0.87	0.056	0.181
6/20/01	6	Charlevoix	45.31426	−85.27962	31	7.46	10.4	3.98	4.08	0.18	1.370	1.839	0.712	55.76	3.69	1.787	0.362
6/17/01	7	Cheboygan	45.41080	−84.26039	31	7.27	9.9	5.24	5.33	0.54	0.239	2.495	0.357	18.57	0.62	0.253	0.125
6/17/01	8	Cheboygan	45.29881	−84.29592	33	7.60	9.6	4.51	4.54	0.13	0.097	1.702	0.671	11.20	1.23	0.021	0.121
6/18/01	9	Cheboygan	45.31683	−84.57888	134	7.85	9.3	3.98	3.54	0.08	0.609	0.883	0.782	25.83	5.12	0.008	0.078
6/17/01	10	Cheboygan	45.29273	−84.27508	75	8.30	10.1	3.28	3.46	0.16	1.762	0.364	0.416	26.60	2.40	0.029	0.022
6/17/01	11	Cheboygan	45.40319	−84.48831	27	7.43	10.1	5.85	5.50	0.27	0.165	1.761	1.456	49.62	6.47	0.065	0.197
6/17/01	12	Cheboygan	45.25739	−84.28306	46	7.67	9.8	4.37	4.18	0.47	0.114	1.667	0.774	17.14	0.97	0.005	0.150
6/17/01	13	Cheboygan	45.35224	−84.30030	98	8.11	10.6	2.64	2.43	0.45	0.726	0.509	0.473	20.87	3.66	0.037	0.067
6/18/01	14	Cheboygan	45.35280	−84.61871	95	7.64	10.1	3.85	3.79	0.13	0.234	1.579	0.613	42.46	0.39	0.474	0.109
6/16/01	15	Cheboygan	45.53204	−84.69454	135	7.96	11.2	3.31	3.18	0.27	0.787	0.681	0.728	29.16	5.89	0.030	0.091
6/18/01	16	Cheboygan	45.36726	−84.50451	43	7.56	8.9	4.80	3.56	0.06	0.429	1.365	1.107	47.57	7.12	0.015	0.157
6/18/01	17	Cheboygan	45.30703	−84.50808	76	8.74	9.3	2.43	2.07	0.03	1.823	0.160	0.122	8.90	1.44	0.029	0.001
6/18/01	18	Cheboygan	45.27999	−84.65240	140	7.41	9.8	5.26	4.51	0.14	0.874	2.236	0.880	223.28	0.88	1.800	0.104
6/17/01	19	Cheboygan	45.40426	−84.49609	51	7.69	9.8	4.34	4.09	0.63	0.670	1.128	1.049	36.32	6.90	0.049	0.211
6/17/01	20	Cheboygan	45.37657	−84.26938	85	7.93	9.6	4.36	3.99	0.15	1.053	1.223	0.934	86.96	11.01	0.417	0.301
6/18/01	21	Cheboygan	45.35960	−84.61980	90	7.60	9.6	3.99	3.47	0.09	0.121	1.437	0.745	25.30	7.08	0.165	0.120
6/18/01	22	Cheboygan	45.37585	−84.71168	72	7.47	9.3	5.28	5.21	0.13	0.256	1.724	1.090	15.65	2.96	0.102	0.189
6/18/01	23	Cheboygan	45.36525	−84.58540	32	7.65	13.2	4.33	3.93	0.07	0.470	1.065	0.864	15.24	6.39	0.016	0.051
6/19/01	24	Emmet	45.36303	−84.90343	87	7.52	10.9	4.74	4.35	0.14	0.169	1.322	0.983	46.55	6.09	0.013	0.097
6/19/01	25	Emmet	45.37619	−84.81049	48	7.68	9.3	3.94	3.46	0.09	0.336	0.983	0.823	30.44	5.85	0.024	0.106
6/19/01	26	Emmet	45.35128	−84.81634	98	7.71	9.1	3.87	3.58	0.11	1.005	0.866	0.630	34.27	7.21	0.019	0.137
6/19/01	27	Emmet	45.39370	−84.88982	79	7.48	9.7	4.46	4.37	0.12	0.099	1.554	0.745	23.91	1.31	0.065	0.101
6/19/01	28	Emmet	45.35091	−85.07566	93	7.45	10.4	4.70	4.44	0.05	0.139	1.774	0.802	21.74	1.02	0.278	0.167
6/19/01	29	Emmet	45.29687	−84.99680	96	7.65	9.1	3.56	3.41	0.08	0.045	1.195	0.564	18.13	0.55	0.022	0.053
6/19/01	30	Emmet	45.40036	−84.74775	110	7.82	11.2	3.81	3.44	0.11	2.475	1.190	1.066	43.48	12.33	1.260	1.130
6/16/01	31	Emmet	45.78382	−84.75579	23	7.37	8.9	5.54	5.66	0.66	0.133	1.924	1.024	26.09	2.61	0.160	0.138
6/16/01	32	Emmet	45.49642	−84.73079	116	7.86	10.4	2.41	2.24	0.33	2.218	2.645	2.765	52.69	47.25	0.535	4.920
6/16/01	33	Emmet	45.61757	−84.95500	180	8.31	8.8	3.26	3.07	0.37	0.900	0.519	0.786	32.74	7.62	0.011	0.038
6/19/01	34	Emmet	45.32630	−84.97309	84	7.65	10.5	3.82	3.38	0.08	0.626	0.921	0.806	18.59	4.95	0.080	0.104
5/21/01	35	Presque Isle	45.34734	−83.78924	75	7.61	9.5	4.73	4.33	0.09	1.227	1.243	0.792	55.50	18.03	0.330	0.148
5/19/01	36	Presque Isle	45.46991	−84.23388	52	7.97	13.0	4.01	3.53	0.20	0.419	0.843	1.113	40.67	6.62	0.007	0.033
5/19/01	37	Presque Isle	45.54341	−84.12759	157	8.37	11.5	2.84	1.83	0.02	8.221	0.516	0.493	9.64	9.00	5.236	1.433
5/21/01	38	Presque Isle	45.30937	−83.55646	12	7.69	10.2	3.86	3.42	0.06	2.562	2.415	1.365	45.27	17.69	2.068	1.993
5/20/01	39	Presque Isle	45.28922	−83.89556	22	7.60	12.3	4.41	4.00	0.07	0.123	1.442	0.832	17.49	24.77	0.015	0.061
5/21/01	40	Presque Isle	45.34579	−83.72984	26	7.54	10.9	4.71	4.26	0.05	1.866	1.290	1.022	35.04	21.68	1.596	0.196
5/20/01	41	Presque Isle	45.46939	−33.89788	102	7.97	8.9	3.46	2.95	0.11	0.770	0.823	0.701	9.49	21.11	0.107	0.048
5/19/01	42	Presque Isle	45.54444	−84.12803	115	8.67	9.0	2.42	2.11	0.02	9.047	0.240	0.176	17.44	3.64	5.084	1.324
5/19/01	43	Presque Isle	45.38859	−84.22247	64	8.05	11.0	2.71	2.44	0.05	0.948	0.838	0.525	35.04	4.19	0.412	0.254
5/20/01	44	Presque Isle	45.24833	−83.74757	66	7.25	9.7	6.08	5.87	1.31	0.187	2.844	0.602	43.48	1.56	0.490	0.193
5/20/01	45	Presque Isle	45.40932	−83.92784	70	7.59	9.2	3.82	3.49	0.32	0.197	1.699	0.781	6.42	0.62	0.293	0.424
5/19/01	46	Presque Isle	45.27320	−84.16710	113	7.72	9.1	4.83	4.39	0.06	1.013	1.018	1.004	49.11	41.66	0.008	0.084

(*continued on next page*)

Table 1 (*continued*)

Date	ID#	County	Latitude	Longitude	Depth (m)	pH	*T* (°C)	Alkalinity (meq/kg)	DIC (mmol/kg)	DOC (mM)	Na (mM)	Ca (mM)	Mg (mM)	*K* (μM)	Sr (μM)	Cl (mM)	SO_4 (mM)
5/20/01	47	Presque Isle	45.29591	−83.97211	62	7.66	10.0	4.18	3.85	0.22	0.200	1.255	0.847	28.13	37.66	0.016	0.078
5/21/01	48	Presque Isle	45.38235	−83.85626	66	7.49	9.7	4.28	3.74	0.19	0.108	1.874	0.467	6.50	3.52	0.006	0.096
5/20/01	49	Presque Isle	45.30293	−83.85064	17	7.42	10.3	5.28	4.78	0.29	0.944	2.595	0.828	35.55	2.57	1.332	0.282
5/20/01	50	Presque Isle	45.26959	−83.69376	32	7.75	11.6	4.33	3.85	0.07	0.618	1.063	1.343	46.29	17.92	0.580	0.330
5/21/01	51	Presque Isle	45.25259	−83.47241	43	7.64	9.6	4.00	3.60	0.17	1.201	1.931	0.894	43.74	5.38	0.683	0.925
10/19/02	52	Presque Isle	45.43333	−84.22500	73	7.16	12.9	1.88			1.183	0.554	0.303	46.55	2.61	0.129	0.329
Michigan glacial drift wells																	
5/21/01	53	Alpena	44.94410	−83.76580	32	7.53	13.9	4.51	4.15	0.10	0.176	1.974	0.785	14.09	0.59	0.627	0.171
5/21/01	54	Alpena	45.03220	−83.71595	16	7.58	10.0	5.86	5.51	1.47	0.256	2.994	0.843	21.38	1.11	1.614	0.235
11/18/03	55	Benzie	44.65000	−86.23330	91	7.83	9.9	3.92	3.61		4.276	2.859	1.962	48.19	28.80	3.051	3.326
11/18/03	56	Benzie	44.60000	−86.22500	135	7.79	9.7	3.95	3.82		0.281	1.176	0.777	21.84	3.30	0.028	0.194
11/18/03	57	Benzie	44.54170	−86.19170	62	7.83	9.2	3.73	3.60		0.129	1.248	0.775	21.54	1.09	0.045	0.256
11/18/03	58	Benzie	44.60000	−86.10000	69	8.10	10.3	3.26	3.01		1.552	0.670	0.456	31.55	3.47	0.436	0.046
6/20/01	59	Charlevoix	45.21673	−84.99740	26	7.80	10.2	3.05	2.99	0.16	0.063	1.215	0.377	30.18	0.11	0.007	0.081
6/20/01	60	Charlevoix	45.21651	−84.75784	90	7.37	9.1	5.37	5.39	0.09	0.103	1.884	1.029	1.94	0.51	0.045	0.166
6/20/01	61	Charlevoix	45.31773	−85.13929	84	7.63	9.9		3.40	0.24	0.080	1.704	0.535	17.39	0.43	0.219	0.111
6/18/01	62	Cheboygan	45.39253	−84.70456	32	8.15	9.9	3.20	2.60	0.12	0.883	0.432	0.736	17.85	5.59	0.010	0.022
6/18/01	63	Cheboygan	45.32054	−84.56939	32	7.66	11.1	4.17	3.91	0.15	0.433	1.158	0.839	28.13	4.88	0.014	0.070
6/18/01	64	Cheboygan	45.42168	−84.58840	77	8.21	8.9	2.80	2.56	0.14	0.761	0.499	0.642	24.45	10.80	0.017	0.077
6/16/01	65	Cheboygan	45.52839	−84.69613	62	8.33	11.8	3.23		0.45	2.179	0.274	0.539	44.76	3.65	0.033	1.103
6/17/01	66	Cheboygan	45.51586	−84.41405	62	8.11	9.2	4.40	5.44	0.64	3.080	0.379	0.258	13.63	3.41	0.020	0.002
6/18/01	67	Cheboygan	45.22446	−84.50644	48	7.45	8.5	4.91	4.59	0.11	0.080	1.759	0.765	13.45	0.35	0.008	0.132
6/17/01	68	Cheboygan	45.64569	−84.45073	24	8.26	10.9	2.05	2.00	0.18	1.309	0.641	0.531	20.46	15.07	0.231	0.582
6/16/01	69	Cheboygan	45.64883	−84.72870	47	7.96	11.9	3.78	3.24	1.39	0.696	0.729	0.971	58.57	14.15	0.009	1.020
10/19/02	70	Cheboygan	45.27500	−84.26667	73	7.87	9.4	3.31			0.697	0.552	0.701	0.00	5.52	0.008	0.009
6/19/01	71	Emmet	45.40282	−84.74938	29	8.03	9.7	3.53	3.22	0.23	0.887	0.492	0.778	27.37	5.60	0.008	0.011
6/16/01	72	Emmet	45.72050	−84.83337	32	7.88	9.4	3.41	3.24	0.83	0.271	0.913	0.662	28.90	12.67	0.019	0.002
6/19/01	73	Emmet	45.37614	−84.75017	38	7.63	9.2	3.68	3.43	0.14	0.075	1.300	0.535	18.54	0.22	0.048	0.101
6/19/01	74	Emmet	45.29119	−84.85983	49	7.59	9.7	4.23		0.37	0.099	1.567	0.506	19.57	0.41	0.016	0.118
6/16/01	75	Emmet	45.61782	−84.96458	80	7.95	9.3	4.41	4.28	0.17	0.417	0.671	1.391	47.32	6.43	0.015	0.048
6/19/01	76	Emmet	45.72050	−84.83337	89	7.81	9.4	3.38	3.15	0.11	0.132	0.953	0.687	3.04	2.83	0.013	0.083
6/16/01	77	Emmet	45.62344	−84.79068		7.93	9.0	3.75	3.65	0.31	0.258	0.968	0.868	40.41	7.18	0.006	0.034
6/16/01	78	Emmet	45.63296	−84.78275		8.02	10.3	3.76	3.51	0.33	0.492	0.973	0.901	31.20	13.12	0.041	0.036
11/18/03	79	Manistee	44.46670	−86.15000		7.72	11.5	3.08	3.05		0.147	1.129	0.709	17.80	0.96	0.377	0.162
5/21/01	80	Montmorency	45.10975	−83.94917	51	7.65	10.0	4.04	3.61	0.13	0.421	1.302	0.635	11.87	3.72	0.020	0.001
10/19/02	81	Montmorency	45.10333	−84.17000	69	6.51	9.9	3.99			0.137	1.629	0.613	0.00	0.70	0.057	0.134
5/19/01	82	Presque Isle	45.32464	−84.20270	72	7.50	10.5	5.75	5.45	0.26	0.159	2.141	0.934	24.66	0.60	0.017	0.186
5/19/01	83	Presque Isle	45.55201	−84.13646	119	8.43	9.8	3.04	2.53	0.10	7.786	0.337	0.442	37.60	8.73	4.513	0.970
5/20/01	84	Presque Isle	45.29600	−83.85151	24	7.49	11.5	5.32	4.68	0.11	0.200	2.695	0.635	74.68	1.03	0.323	0.141
5/19/01	85	Presque Isle	45.49473	−84.17473	49	8.11	9.2	3.15	2.73	0.11	0.457	0.614	0.730	28.39	2.68	0.008	0.003
5/19/01	86	Presque Isle	45.54341	−84.12759	80	8.72	14.3	3.71	3.24	0.07	5.307	0.131	0.112	3.40	1.72	1.587	0.217
5/19/01	87	Presque Isle	45.46042	−84.22196	18	8.09	17.6	3.38	2.88	0.25	0.679	0.651	0.796	19.00	6.68	0.007	0.023
5/21/01	88	Presque Isle	45.36930	−83.78025	15	7.26	9.5	5.54	5.17	0.43	0.202	2.360	0.763	38.62	0.58	0.312	0.172
5/19/01	89	Presque Isle	45.32028	−84.24479	31	7.58	11.6	5.22	5.10	0.11	0.121	2.388	0.836	17.39	0.60	0.114	0.124

Indiana bedrock wells																	
7/28/01	90	Allen	41.24511	−84.84644	47	7.35	12.5	7.26	7.70	0.96	2.353	3.144	5.390	54.99	123.26	0.140	5.871
7/28/01	91	Allen	45.30937	−83.55646	69	7.16	16.0	8.63	8.28	1.90	0.853	3.892	2.806	37.09	23.05	0.332	2.567
7/28/01	92	Allen	41.13832	−84.91599	79	7.26		6.28	7.86	0.18	1.301	2.769	1.991	99.24	57.52	1.013	1.747
7/28/01	93	Allen	41.25771	−85.01974		7.28	12.4	8.52	6.23	0.16	1.161	2.570	2.432	63.43	52.04	0.226	1.169
7/28/01	94	Allen	41.15444	−84.88053	55	7.37	13.4	6.40	6.39	0.13	1.670	1.924	2.687	67.78	102.37	0.369	2.232
7/27/01	95	Allen	41.20951	−85.20954	78	7.47	12.2	6.92	6.40	0.30	0.713	1.704	1.531	48.08	48.85	0.033	0.146
7/24/01	96	Benton	40.69581	−87.41934	91	7.53	13.9	6.15	5.60	0.12	1.592	1.390	1.062	82.61	3.88	0.044	0.155
7/24/01	97	Benton	40.72206	−87.40646	37	7.75	13.9	6.41	5.11	0.10	4.611	0.778	0.605	103.07	10.10	0.129	0.638
7/26/01	98	Fulton	40.91141	−86.39124	75	7.40	15.4	6.38	5.75	0.13	0.252	2.345	1.119	48.08	2.70	0.073	0.227
7/26/01	99	Jasper	41.15362	−87.15221	26	7.39	14.9	4.66	4.20	0.25	0.465	1.761	0.815	20.95	5.70	0.484	0.181
7/26/01	100	Jasper	41.07054	−86.98573	56	7.47	16.0	9.02	8.92	1.94	3.362	1.991	1.234	55.76	9.31	0.380	0.485
7/26/01	101	Jasper	41.11556	−87.05144	20	7.77	14.4	4.31	5.52	0.31	1.970	1.173	0.621	2.53	20.31	0.030	0.699
7/26/01	102	Kosciusko	41.07623	−85.86982	101	7.69	12.3	5.26	4.62	0.12	0.931	1.295	0.811	55.76	13.47	0.102	0.017
7/26/01	103	Miami	40.92002	−86.07819	110	7.80	12.7	6.50	4.85	0.32	1.875	1.297	1.024	29.67	11.87	0.336	0.013
7/24/01	104	Newton	40.76870	−87.31559	64	7.56	15.3	7.58	6.97	0.78	5.611	1.243	1.432	192.59	3.97	2.105	0.675
7/24/01	105	Newton	40.87732	−87.46014	56	7.73	14.7	11.73	11.30	5.29	11.744	0.434	0.448	194.64	5.62	1.895	0.109
7/24/01	106	Newton	40.99869	−87.28417	30	7.79	14.2	4.60	4.02	0.21	2.549	1.013	0.642	38.88	9.92	0.093	0.733
7/24/01	107	Newton	40.96001	−87.41357	85	7.47	17.2	6.02	5.42	0.23	2.040	0.993	1.062	164.71	7.97	0.418	0.327
7/26/01	108	Pulaski	41.10092	−86.80801	67	7.77	13.8	3.68	3.59	0.29	0.831	0.898	0.555		3.10	0.018	0.001
7/26/01	109	Pulaski	41.05583	−86.66837	69	8.28	13.8	3.03	3.13	0.14	3.789	0.312	0.436	31.97	8.63	1.565	0.395
7/26/01	110	Pulaski	41.08128	−86.56327	66	7.82	14.3	4.49	4.12	0.11	0.861	1.063	0.728	45.78	10.64	0.078	0.008
7/27/01	111	Whitley	41.13247	−85.47361		7.56	12.1	6.80	6.35	0.10	0.774	2.003	1.333	74.17	56.15	0.254	0.198
7/27/01	112	Whitley	41.19356	−85.46305	116	7.60	12.1	5.88	5.69	0.29	1.405	1.218	1.103		34.35	0.027	0.099
7/27/01	113	Whitley	41.12784	−85.39458	85	7.56	12.1	7.04	5.81	0.18	0.874	1.834	1.407	72.89	53.53	0.071	0.211
Indiana glacial drift wells																	
7/28/01	114	Allen	41.68780	−87.48836		7.16	15.7	7.60	6.80	1.05	0.331	3.443	1.555	23.33	3.91	0.836	0.911
7/28/01	115	DeKalb	41.44050	−84.85159	42	7.58	14.6	6.67	4.93	0.27	0.500	2.298	1.695	53.97	62.66	0.211	0.821
7/28/01	116	DeKalb	41.50714	−84.89140	69	7.35	12.5	6.55	6.44	0.50	0.478	2.493	1.317	39.39	20.77	0.104	0.603
7/28/01	117	DeKalb	41.27791	−84.84610	66	7.64	13.0	6.34	6.04	0.19	1.396	1.724	2.028	54.99	89.02	0.061	1.241
7/24/01	118	Newton	41.03398	−87.37532	18	7.33	15.9	3.34	3.07	0.47	0.224	1.906	0.403	31.97	2.64	0.293	0.667
Ohio bedrock wells																	
5/29/03	119	Fulton	41.56725	−83.95970	27	7.48	13.9	4.67	4.24	0.34	16.167	2.384	2.033	152.95	316.14	21.914	0.000
5/29/03	120	Fulton	41.62770	−84.02320	55	7.61	13	6.31	5.75	0.36	19.123	1.202	0.934	157.90	75.44	18.267	0.000
5/30/03	121	Fulton	41.60595	−84.04386	53	7.42	13.4	9.75	10.88	0.38	8.885	0.806	0.531	123.45	53.98	2.932	0.000
5/30/03	122	Fulton	41.69743	−84.16092	55	7.44	12.9	4.61	4.24	0.32	6.794	3.239	1.638	65.35	49.99	3.046	4.667
5/30/03	123	Fulton	41.62297	−83.95480	52	7.01	13.8	16.22	15.88	0.29	14.370	1.770	0.918	181.61	136.96	4.735	0.000
5/30/03	124	Fulton	41.59573	−83.96992	38	7.45	13	8.09	7.45	0.30	12.449	1.489	1.251	140.59	110.36	10.237	0.000
5/30/03	125	Fulton	41.66838	−83.87959	66	7.56	12.6	10.14	9.12	0.22	8.997	0.605	0.424	110.84	82.74	2.070	0.000
5/30/03	126	Fulton	41.66288	−83.99708	53	7.84	12.6	3.45	2.95	0.49	89.579	7.106	4.649	692.31	496.46	115.935	0.000
5/29/03	127	Lucas	41.45901	−83.80707	18	7.73	13.2	3.71	3.58	0.47	1.968	0.442	0.394	20.87	67.56	0.107	0.000
5/29/03	128	Lucas	41.48062	−83.83299	34	7.76	12.6	3.21	3.07	0.40	2.232	0.418	0.373	22.69	75.90	0.118	0.411
5/29/03	129	Lucas	41.49335	−83.84881	30	8.00	12.6	3.39	3.10	0.33	2.761	0.261	0.241	36.07	77.61	0.217	0.212
5/29/03	130	Lucas	41.50159	−83.88096	52	7.53	13.8	6.02	4.72	0.26	2.178	0.921	0.802	84.66	127.82	0.174	0.070

(*continued on next page*)

Table 1 (*continued*)

Date	ID#	County	Latitude	Longitude	Depth (m)	pH	*T* (°C)	Alkalinity (meq/kg)	DIC (mmol/kg)	DOC (mM)	Na (mM)	Ca (mM)	Mg (mM)	*K* (μM)	Sr (μM)	Cl (mM)	SO_4 (mM)
Ohio glacial drift wells																	
5/29/03	131	Fulton	41.62843	−84.03520	52	7.52	13.1	9.05	8.24	0.72	32.468	2.307	1.967	200.22	152.93	34.371	0.000
5/30/03	132	Fulton	41.65530	−84.08899	6	7.49	10.5	3.51	3.30	0.84	0.165	1.553	0.564	23.89	2.74	0.241	0.420
5/30/03	133	Fulton	41.68145	−84.11078	53	8.13	12.7	2.66	2.34	0.40	10.867	0.587	0.440	58.95	75.67	10.249	0.000
5/30/03	134	Fulton	41.66919	−84.09346	54	8.15	12.9	1.79	1.56	0.38	20.753	2.932	1.995	124.05	257.93	30.102	0.000

4. Results and discussion

4.1. Salinity structure of fluids in Silurian-Devonian aquifers

Prolific drilling for hydrocarbons in Silurian-Devonian strata in the Michigan and Illinois basins has provided important sampling points for fluid chemistry in the deeper basin sections. Groundwaters from Silurian-Devonian carbonate aquifers presented in this study provide key constraints on the meteoric water endmembers along the shallow basin margins, and the freshwater–saline water mixing zone. Integrating our geochemical database of basinal brines and groundwaters, a contour map was created of the salinity structure in the Silurian-Devonian carbonate regional aquifer system in the Midcontinent region (Fig. 4).

The Cl^- concentration of fluids in Silurian-Devonian carbonates in the Michigan Basin rapidly increases from less than 0.5 M to greater than 5.0 M, less than 100 km basinward of the carbonate subcrop and less than 0.5 km depth. In contrast, formation waters in Illinois Basin Silurian-Devonian carbonates are much more dilute, containing less than 3.0 M Cl^- at depths greater than 1.25 km. The spatial pattern of salinity illustrates the influx of meteoric waters into the carbonate subcrop along the basin margins and mixing with basinal brines at depth. Major differences in the salinity of Silurian-Devonian brines in the Michigan and Illinois basins likely controlled the extent of glacial meltwater invasion (McIntosh and Walter, 2005). Paleowaters infiltrated to depths of nearly 1 km along the eastern margin of the Illinois Basin. The north-to-south orientation of this salinity depression corresponds to the major axis of the Laurentide Ice Sheet as it advanced and retreated. Similar salinity patterns and fluid chemistry in overlying Upper Devonian shales, indicate that dilute waters migrated into the shales through the underlying Devonian carbonate aquifers. This circulation of meteoric waters through the fractured, organic-rich shales has generated relatively recent economic reservoirs of microbial methane along the shallow margins of the Illinois and Michigan basins (Martini et al., 1998; McIntosh et al., 2002).

4.2. Sources of meteoric water in Paleozoic aquifers

Large-scale infiltration of Pleistocene glacial meltwaters into the Great Lakes region was first documented in the Cambrian-Ordovician aquifer system in the Illinois Basin, using the isotopically depleted $\delta^{18}O$ and δD values for glacial meltwaters versus modern precipitation (Siegel and Mandle, 1984; Siegel, 1991; Stueber and Walter, 1994) (Fig. 5a). New elemental and isotope geochemical data presented in this study show that this recharge of $\delta^{18}O$ and δD depleted waters was regionally extensive and also pervasive in the Silurian-Devonian carbonate aquifer system in the Michigan and Illinois basins (Fig. 5b). The $\delta^{18}O$ values of modern precipitation in this area range from −11.0 to

Table 2
Minor ion chemistry, saturation indices, and isotope chemistry of groundwaters in bedrock and glacial drift aquifers

ID#	Ba (μM)	B (μM)	Mn (μM)	Fe (μM)	Si (μM)	Al (μM)	NO_3 (μM)	Br (μM)	LogPCO_2 (atm)	SI[a] Calcite	SI[b] Dolomite	$\delta^{18}O$ H_2O (‰)	δD H_2O (‰)	$\delta^{13}C$ DIC (‰)	$^{87}Sr/^{86}Sr$	$\delta^{34}S$ SO_4 (‰)	$\delta^{18}O$ SO_4 (‰)	Tritium units	$a^{14}C$ (pmc)[c]
Michigan bedrock wells																			
1	0.84	5.92	BD[d]	1.59	156.31	1.89	BD	0.00	−2.24	−0.01	−0.10	−12.77	−87.90	−7.20					
2	0.21	17.21	BD	0.54	150.61	1.56	BD	0.00	−3.29	0.30	0.25	−13.01	−89.07	−12.04	0.70835	12.08			
3	0.91	0.83	0.15	9.78	191.56	4.74	BD	0.00	−2.20	0.10	−0.14	−12.08	−80.64	−10.75					
4	0.10	38.95	BD	0.43	158.44	1.11	1.10	0.00	−3.87	0.05	−0.06	−13.06	−85.00	−12.33		22.92			
5	0.39	0.65	BD	6.21	239.27	3.97	3.31	0.00	−2.02	0.11	−0.02								
6	0.89	3.52	BD	0.50	83.67	4.26	24.69	0.00	−2.13	0.02	−0.19	−8.08	−57.79	−8.80	0.70870	3.58	7.75		
7	0.11	1.30	BD	1.25	70.50	3.67	BD	0.00	−1.81	0.08	−0.36								
8	0.66	0.83	BD	6.79	194.05	5.04	BD	0.00	−2.21	0.19	−0.03								
9	0.73	4.35	BD	3.22	257.78	4.63	BD	0.00	−2.51	0.11	0.06	−12.82	−87.54	−10.61					
10	0.36	9.99	BD	1.65	70.14	BD	BD	0.00	−3.05	0.13	0.15								
11	0.38	2.04	BD	4.30	147.05	3.11	1.28	0.00	−1.93	0.12	0.08								
12	0.39	BD	BD	0.91	192.27	3.26	4.18	0.00	−2.30	0.24	0.06								
13	0.58	4.44	BD	0.88	133.16	4.48	BD	0.00	−2.95	0.01	−0.01								
14	0.14	0.93	BD	0.64	46.64	1.74	194.34	0.00	−2.32	0.15	−0.07	−12.67	−84.54	12.80					
15	0.20	3.33	BD	1.88	108.95	BD	BD	0.00	−2.70	0.07	0.10	−12.90	−86.07	−9.84	0.70913	7.01			
16	0.23	4.26	BD	0.75	131.74	0.85	1.30	0.38	−2.15	0.06	−0.01								
17	0.24	11.66	BD	0.30	163.43	0.41	BD	0.00	−3.62	0.07	0.00	−12.19	−83.24	−9.50	0.70834				
18	BD	1.85	BD	1.02	127.47	3.04	192.63	0.00	−1.96	0.15	−0.06	−13.03	−87.68	−12.99		6.85		13.2 ± 1.1	
19	0.42	4.53	BD	1.58	96.85	2.78	5.89	0.00	−2.32	0.08	0.06								
20	0.58	2.87	BD	2.90	118.21	1.19	BD	0.00	−2.55	0.34	0.27	−12.86	−87.04	−5.68					
21	1.27	0.37	0.18	9.35	149.54	4.78	BD	0.00	−2.26	0.07	−0.09	−12.73	−86.67	−11.91					
22	0.47	0.09	0.29	10.12	227.52	BD	BD	0.00	−2.01	0.11	−0.01	−12.63	−83.75	−13.21	0.70910				
23	0.01	7.77	BD	0.68	163.79	3.82	9.32	0.00	−2.28	0.09	0.09	−12.47	−81.62	−12.48					
24	0.71	2.96	BD	3.58	117.85	3.37	BD	0.00	−2.10	0.04	−0.02								
25	0.53	1.30	BD	3.49	219.33	1.00	0.95	0.00	−2.34	−0.02	−0.08	−13.21	−89.05	−9.29					
26	0.90	3.24	BD	1.59	137.44	3.60	BD	0.00	−2.38	−0.05	−0.14	−13.14	−88.82	−5.70					
27	0.27	0.37	BD	6.75	168.77	2.67	BD	0.00	−2.09	0.03	−0.14	−12.79	−86.20	−11.60					
28	0.87	0.83	BD	0.47	87.95	3.63	68.60	0.00	−2.05	0.08	−0.09	−12.26	−82.98	−11.70					
29	0.16	0.93	BD	0.57	117.14	4.63	33.68	0.00	−2.35	0.00	−0.19	−12.91	−87.01	−10.86					
30	0.60	5.09	0.33	11.66	157.02	4.86	BD	0.00	−2.51	0.15	0.14	−12.96	−90.14	−6.23	0.70872	26.12	14.38	<0.8 ± 0.5	5.76
31	0.12	0.56	BD	0.77	117.50	2.78	8.31	0.00	−1.89	0.07	−0.10	−11.38	−81.04	−13.70	0.70895	6.36	6.16		
32	BD	7.77	BD	11.51	188.00	3.45	BD	0.00	−2.77	0.20	0.20	−13.44	−87.90	−5.67	0.70909	25.97	11.29		
33	0.09	1.39	BD	18.62	176.60	BD	0.00	0.00	−3.06	0.25	0.32								
34	0.80	4.44	BD	3.26	157.02	BD	BD	0.00	−2.32	−0.07	−0.10								
35	0.14	3.79	BD	3.56	187.28	6.04	BD	0.00	−2.19	0.07	−0.14	−11.93	−82.04	−6.12					
36	0.22	2.96	BD	2.54	214.34	0.52	1.96	0.00	−2.38	0.27	0.24	−12.12	−83.15	−7.93	0.70931	8.99	4.65	<0.8 ± 0.5	
37	BD	13.88	BD	0.93	133.16	7.34	3.02	2.31	−3.58	0.18	0.07	−14.21	−98.42	−5.75	0.70893	25.66	12.19	<0.8 ± 0.5	4.39
38	0.66	5.46	0.05	6.21	139.22	4.30	2.55	1.08	−2.88	0.27	0.03			−6.11	0.70875	17.87	11.54		
39	0.65	1.94	BD	6.71	166.99	7.00	BD	0.00	−1.73	0.15	−0.06	−11.49	−81.12	−8.76	0.70807				
40	1.38	9.16	0.09	1.92	142.06	3.30	4.13	0.00	−2.28	0.02	−0.13	−11.20	−75.15	−7.68	0.70860				
41	1.06	4.63	BD	2.29	172.68	0.07	2.59	0.00	−2.30	0.14	−0.01	−12.08	−82.32	−8.45					
42	0.35	15.54	BD	0.63	111.09	2.93	2.91	1.82	−2.13	0.04	−0.14	−14.98	−103.40	−6.15					
43	BD	5.18	BD	1.74	122.12	7.26	BD	0.00	−2.38	0.15	−0.05	−13.72	−94.33	−3.36	0.70911	4.34	6.67	<0.8 ± 0.5	3.14
44	0.33	1.20	0.64	5.77	147.40	2.19	2.38	0.00	−2.31	0.16	−0.29	−10.43	−71.84	−12.49					
45	BD	3.61	BD	0.36	124.26	6.86	139.50	0.00	−2.01	0.09	−0.19								
46	1.56	5.55	BD	4.62	215.41	3.63	2.65	0.00	−3.22	0.11	−0.01	−11.41	−78.92	−9.70	0.70807	7.79		<0.8 ± 0.5	

(*continued on next page*)

Table 2 (*continued*)

ID#	Ba (μM)	B (μM)	Mn (μM)	Fe (μM)	Si (μM)	Al (μM)	NO_3 (μM)	Br (μM)	Log PCO_2 (atm)	SI[a] Calcite	SI[b] Dolomite	$\delta^{18}O$ H_2O (‰)	δD H_2O (‰)	$\delta^{13}C$ DIC (‰)	$^{87}Sr/^{86}Sr$	$\delta^{34}S$ SO_4 (‰)	$\delta^{18}O$ SO_4 (‰)	Tritium units	$a^{14}C$ (pmc)[c]
47	0.91	4.26	0.02	2.08	169.48	BD	BD	0.00	−2.14	0.10	−0.10	−10.37	−74.48	−5.26	0.70804				
48	0.50	0.93	BD	8.45	168.41	6.78	2.02	0.00	−2.87	0.11	−0.30	−10.81	−74.86	−10.38					
49	0.55	2.04	BD	0.56	150.61	6.49	456.08	0.00	−2.31	0.23	−0.12	−11.67	−79.37	−11.97					
50	0.18	7.86	0.11	1.06	137.08	2.30	BD	0.17	−1.79	0.13	0.08	−12.09	−81.54	−5.49					
51	0.32	2.96	0.20	43.51	130.67	BD	1.61	0.29	−2.13	0.18	−0.09	−11.42	−77.22	−8.02					
52		BD	0.02	BD	117.14	14.16	4.17	0.00	−2.13	−1.02	−1.11								
Michigan glacial drift wells																			
53	0.42	2.13	BD	0.41	184.43	4.34	97.23	0.88	−2.13	0.23	−0.05								
54	BD	2.78	2.38	68.40	228.23	9.38	0.76	1.89	−3.42	0.48	0.10	−10.67	−72.65	−12.15					
55	0.20	14.96	BD	13.02	214.85	0.21	0.00	16.74	−2.53	0.43	0.34	−7.75	−55.10	−7.97	0.70821	23.30	14.42		
56	0.17	3.16	BD	3.68	199.16	0.46	0.00	0.00	−2.46	0.17	0.07								
57	0.11	1.44	BD	17.47	142.77	0.44	0.00	0.00	−2.52	0.20	0.07	−12.34	−79.94	−13.31	0.70899				
58	0.06	15.20	BD	0.48	184.34	0.51	73.75	0.00	−2.85	0.18	0.09								
59	0.47	0.83	BD	0.25	56.26	3.48	36.95	0.00	−2.58	0.12	−0.14								
60	0.50	0.28	BD	0.77	126.76	2.52	59.07	0.00	−1.90	0.05	−0.11	−12.94	−87.54	−13.77	0.70881	1.49	1.81		
61	0.14	0.00	0.11	0.20	76.20	0.89	384.40	0.00	−2.60	−0.12	−0.38								
62	0.48	5.37	BD	1.36	162.36	1.85	6.53	0.00	−2.91	0.04	0.14	−12.27	−84.00	−9.56					
63	0.29	1.85	BD	0.48	263.84	1.59	6.17	0.00	−2.30	0.09	0.03								
64	0.68	3.61	BD	0.79	168.41	0.37	BD	0.00	−3.02	0.08	0.11	−12.65	−84.86	−9.82					
65	0.14	9.25	BD	0.29	148.48	BD	5.09	0.00	−3.08	0.04	0.21								
66	0.37	14.15	BD	1.79	380.98	2.71	5.26	0.00	−2.72	0.05	−0.05								
67	0.16	0.46	0.36	3.74	137.08	5.52	3.51	0.00	−2.03	0.07	−0.14								
68	0.94	4.63	BD	0.90	84.74	0.44	BD	0.00	−3.21	0.11	0.07	−12.68	−83.86	−7.86	0.70865	22.34	13.12		
69	0.09	2.68	BD	0.30	162.36	2.08	BD	0.00	−2.64	0.15	0.24	−11.74	−78.72	−10.83	0.70926				
70		BD	BD	BD	138.15	BD	BD	0.00	−2.61	−0.13	−0.09								
71	0.39	5.55	BD	2.35	178.03	0.44	7.29	0.00	−2.75	0.01	0.10								
72	0.27	1.48	BD	7.91	130.32	0.33	BD	0.00	−2.61	0.10	0.02	−11.88	−80.93	−12.70					
73	0.07	1.11	BD	0.91	58.39	5.19	40.60	0.00	−2.33	0.03	−0.18			−12.16					
74	0.28	0.46	BD	0.32	128.89	0.37	32.01	0.00	−2.23	0.13	−0.13								
75	0.34	3.24	BD	2.17	190.13	BD	BD	0.00	−2.57	0.12	0.26								
76	0.53	0.65	BD	0.68	104.68	2.30	71.22	0.00	−2.54	0.05	−0.04	−12.79	−84.41	−12.57		2.90	4.58	31.5 ±2.2	
77	0.29	1.67	BD	0.72	81.18	2.22	7.72	0.00	−2.62	0.20	0.16			−10.78					
78	0.25	1.02	0.31	1.81	155.24	6.86	3.44	0.00	−2.71	0.31	0.29	−12.60	−83.79	−11.00	0.70883	6.90	7.98	<0.8 ± 0.5	42.26
79	0.06	4.72	BD	BD	134.11	0.45	126.16	8.37	−2.49	0.01	−0.07	−12.21	−79.90	−12.21					
80	0.48	2.41	BD	11.05	252.08	2.45	BD	0.00	−1.97	0.10	−0.16	−10.87	−78.26	−11.62					
81		BD	0.36	2.74	184.79	8.49	BD	0.00	−1.17	−0.96	−1.18								
82	BD	0.74	BD	0.86	220.75	7.30	2.66	0.00	−2.63	0.29	0.00	−12.00	−84.48	−12.28	0.70909				
83	0.44	15.54	BD	0.61	139.57	2.85	BD	1.89	−3.20	0.08	0.03	−13.49	−94.22	−3.41		26.21	12.13		
84	0.12	0.74	BD	0.52	139.93	0.56	684.15	0.00	−2.22	0.36	−0.06								
85	BD	4.53	BD	0.39	194.76	7.34	0.37	0.00	−2.69	0.13	0.05	−10.87	−79.42	−7.52	0.71035				
86	BD	29.42	BD	0.27	118.21	1.85	BD	0.00	−2.39	0.15	0.04								
87	0.12	4.44	BD	1.33	207.93	4.67	0.31	0.12	−2.04	0.29	0.27								
88	0.37	1.30	0.95	2.01	143.49	4.97	3.67	0.38	−2.82	0.06	−0.30								
89	0.04	2.41	BD	0.72	196.90	3.04	467.11	0.00	−2.08	0.39	0.06	−11.57	−85.24	−11.53					
Indiana bedrock wells																			
90	0.32	37.93	1.09	32.23	341.81	5.19	1.46	1.66	−1.78	0.23	0.25	−8.06	−51.78	−15.52	0.70854	−7.27	6.79	<0.8 ± 0.5	42.11

91	BD	3.24	BD	75.74	459.30	4.34	0.00	1.75	−1.50	0.33	0.18	−8.35	−52.83	−14.67	0.70873	−9.35	5.21		
92	BD	12.12	BD	27.75	147.76	2.33	1.33	1.56							0.70854				74.3[e]
93	0.11	11.29	BD	68.94	384.53	5.26	1.24	0.92	−1.63	0.26	0.15								
94	1.07	28.86	0.55	0.79	258.85	3.11	2.92	1.96	−1.84	0.10	0.08	−8.67	−56.02	−16.02	0.70854	−2.02	10.57		
95	1.59	8.60	0.56	26.86	356.06	BD	1.57	0.82	−1.90	0.25	0.13								
96	BD	26.18	0.36	2.78	158.80	2.89	1.58	BD	−2.01	0.21	0.07	−7.09	−44.65	−8.79	0.70963	4.33			
97	0.03	131.36	0.24	2.99	151.32	0.26	1.63	1.43	−2.21	0.18	0.04	−6.28	−42.53	−15.93	0.70881	15.76		1.3 ±0.6	
98	1.92	2.13	1.00	38.50	322.94	5.56	2.42	1.44	−1.86	0.33	0.09								
99	0.42	10.45	0.31	1.93	241.41	BD	1.17	BD	−1.98	0.08	−0.17	−7.51	−49.97	−9.36					
100	BD	83.81	0.66	11.50	300.86	1.26	54.60	48.34	−1.79	0.45	0.28	−7.70	−49.85	−20.44		57.07	16.08		
101	0.82	62.16	0.35	0.38	211.85	3.52	0.52	0.69	−2.40	0.23	0.01								
102	3.80	7.77	0.64	53.54	275.23	5.71	1.32	BD	−2.23	0.27	0.07								
103	2.44	21.46	0.67	42.62	219.33	1.85	1.08	2.36	−2.25	0.45	0.31	−7.74	−49.00	−12.61					
104	0.44	123.03	BD	0.14	338.61	0.48	102.11	3.28	−1.95	0.25	0.21	−7.21	−46.90	−10.75		11.925	4.08		
105	0.58	311.75	0.15	0.25	137.44	2.15	0.37	4.76	−1.93	0.14	0.07	−9.55	−66.24	−1.96	0.70883	22.02		<0.8 ± 0.6	
106	0.34	94.36	0.24	0.41	198.32	2.19	1.69	1.42	−2.39	0.21	0.02	−6.76	−44.39	−15.92		15.16	13.46	<0.8 ± 0.6	7.56
107	3.28	69.75	0.22	0.36	141.35	5.04	2.51	2.70	−1.95	0.04	−0.01	−15.28	−107.89	−12.98	0.70897	13.09	−9.30	<0.8 ± 0.5	0.12
108	0.52	15.82	0.11	1.18	247.10	BD	1.13	BD	−2.46	0.09	−0.10	−7.52	−49.75	−12.09					
109	0.61	221.09	0.22	0.25	135.30	3.41	0.00	8.02	−3.05	0.01	0.00								
110	1.57	16.10	0.56	3.99	236.42	0.30	5.37	BD	−2.43	0.29	0.13								
111	0.58	8.51	1.64	68.94	332.91	3.89	1.80	1.70	−2.00	0.39	0.21								
112	1.66	14.15	0.40	12.78	285.20	5.56	4.61	BD	−2.09	0.18	0.06	−7.39	−49.07	−13.78		22.19	13.42		
113	7.14	10.18	0.58	35.45	340.75	4.97	1.48	BD	−1.98	0.37	0.22								
Indiana glacial drift wells																			
114	1.27	BD	BD	51.21	366.73	3.93	1.61	1.63	−2.03	0.28	0.03								
115	3.08	6.57	BD	32.23	337.18	4.30	1.38	BD	−2.03	0.47	0.33	−8.57	−55.19	−13.73	0.70845	−3.00 2.06			
116	2.56	2.31	1.35	42.97	325.79	BD	2.21	BD	−1.80	0.25	0.02	−8.61	−57.30	−13.16		1.1 ±0.6			
117	0.58	20.17	BD	22.38	279.50	2.67	1.17	1.57	−2.11	0.35	0.30	−7.78	−51.43	−15.02					
118	0.29	2.13	2.71	53.72	366.74	BD	15.86	32.64	−2.06	−0.08	−0.49	−8.19	−52.52	−10.23	0.70899				
Ohio bedrock wells																			
119	9.65	81.32	1.32	30.30	184.12		24.90	47.53	−2.12	0.15	0.04	−16.35	−110.6	19.51					
120	6.51	69.76	0.37	29.53	216.88		0.00	46.11	−2.14	0.10	−0.04								
121	1.59	79.65	4.46	134.44	157.42		0.00	12.95	−1.71	0.01	−0.16	−17.17	−124.78	16.20	0.70836			<0.8 ± 0.5	
122	0.97	56.07	4.79	52.52	232.13		0.00	0.00	−2.08	0.18	−0.06	−11.54	−78.06	−12.23					
123	1.79	104.63	1.89	52.81	279.53		0.00	17.61	−1.10	0.11	−0.12	−16.06	−115.08	23.49					
124	5.30	88.04	0.60	30.50	253.05		0.00	29.55	−1.84	0.18	0.06	−15.42	−111.68	22.23	0.70842			<0.8 ± 0.5	4.14
125	1.33	79.79	0.38	3.54	201.80		37.67	0.00	−1.84	0.04	−0.13								
126	47.72	72.77	1.17	7.92	98.92		0.00	261.08	−2.68	0.61	0.45	−17.27	−124.53	15.91				1.1 ± 0.6	
127	3.85	78.35	0.00	0.13	229.34		0.00	0.00	−2.42	−0.26	−0.37	−7.34	−47.66	−20.48					
128	2.24	77.69	0.10	1.27	217.83		0.00	0.00	−2.52	−0.35	−0.46	−7.86	−52.83	−17.60					
129	0.74	95.18	0.00	0.00	187.79		0.00	0.00	−2.74	−0.27	−0.39								
130	0.99	110.20	0.00	0.00	168.20		0.00	0.00	−2.02	0.03	−0.08	−8.31	−55.8	−5.26	0.70833			<0.8 ± 0.5	4.60
Ohio glacial drift wells																			
131	14.26	85.99	0.33	71.34	245.28		0.00	107.46	−1.89	0.39	0.28	−17.8	−128.61	16.22					
132	0.26	7.52	0.21	0.00	139.47		0.00	0.00	−2.21	−0.06	−0.39	−8.98	−56.54	−12.75	0.70897			9.4 ± 0.9	

(*continued on next page*)

Table 2 (*continued*)

ID#	Ba (μM)	B (μM)	Mn (μM)	Fe (μM)	Si (μM)	Al (μM)	NO_3 (μM)	Br (μM)	$LogPCO_2$ (atm)	SI[a] Calcite	SI[b] Dolomite	$\delta^{18}O$ H_2O (‰)	δD H_2O (‰)	$\delta^{13}C$ DIC (‰)	$^{87}Sr/^{86}Sr$	$\delta^{34}S$ SO_4 (‰)	$\delta^{18}O$ SO_4 (‰)	Tritium units	$a^{14}C$ (pmc)[c]
133	2.05	67.20	0.12	2.67	190.41		0.00	28.19	−2.99	0.02	−0.13								
134	14.33	61.40	1.62	48.91	163.29		0.00	67.04	−3.23	0.45	0.28	−18.11	−132.88	−2.43					

[a] Saturation index for calcite = Log (IAP/K_T).
[b] Saturation index for dolomite = Log (IAP/K_T)$^{1/2}$.
[c] Percent modern carbon.
[d] BD, below detection limit.
[e] Carbon-14 analysis from Eberts and George (2000).

−4.5‰ (Clayton et al., 1966; Coplen and Kendall, 2000; Eberts and George, 2000; IAEA/WMO, 2001), whereas estimated $\delta^{18}O$ values for glacial meltwater in the Great Lakes region range from −25 to −11‰ (Clayton et al., 1966; McNutt et al., 1987; Long et al., 1988; Dettman et al., 1995; Husain et al., 2004). Together, the stable isotope chemistry and salinity patterns suggest that Pleistocene glaciation reorganized regional-scale groundwater flow and introduced geochemically distinct fluids to great depths in Paleozoic aquifers. Since the Late Pleistocene, these glacial meltwaters have been extensively altered by water–rock reactions, fluid mixing, and biogeochemical processes.

4.3. Major ion chemistry and sources of salinity

The ternary diagrams in Fig. 6 illustrate the major elemental composition of groundwaters in Silurian-Devonian and overlying glacial drift aquifers along the margins of the Michigan and Illinois basins. The majority of groundwaters are $CaMgHCO_3$-type waters, predominately located in recharge areas and unconfined aquifers. $CaMgSO_4$-, $NaHCO_3$-, and NaCl-type waters are located downgradient in confined aquifers beneath lake-bed clays or Upper Devonian shales, likely altered by water–rock and microbial interactions, and mixing with saline fluids. Groundwaters in the four different water-type groups have distinct elemental and isotope geochemistries, and the four groups are used throughout the paper to investigate the hydrology and geochemical evolution of fluids.

Groundwaters dominated by NaCl may have evolved from halite dissolution in evaporite-bearing Silurian-Devonian aquifers along the margins of the Michigan and Illinois basins and/or from mixing with saline formation waters. Na–Cl–Br relations are utilized to delineate the sources of salinity (Fig. 7), which may have important implications for groundwater flow paths and sources of solutes. Formation waters in Silurian-Devonian carbonates, down dip in the Illinois and Michigan basins, are highly saline NaCaClBr-rich fluids that evolved from subaerially evaporated seawater and water–rock reactions (Stueber and Walter, 1991; Wilson and Long, 1993b). Figs. 7a and b show the mixing trends for meteoric waters and Silurian-Devonian brines in the Illinois Basin and Upper Devonian Antrim Shale formation waters from the southern margin of the Michigan Basin. These fluids were chosen as plausible basinal brine endmembers, which mixed with dilute groundwaters along the basin margins.

The majority of $CaMgHCO_3$, $CaMgSO_4$, and $NaHCO_3$ groundwaters have low Cl^-, Br^-, and Na^+ concentrations, plotting near the meteoric water endmember values in Figs. 7c and d. Relatively dilute NaCl groundwaters from the northern margin of the Michigan Basin also plot near the origin in Figs. 7c and d. These Br^- poor waters primarily derived their salinity from meteoric water dissolution of halite in evaporite-bearing carbonate aquifers. In contrast, NaCl groundwaters along the southern margin of the

Table 3
Mass transfer of phases calculated using NETPATH, in mmol/kg water

Cross-section	Initial well	Final well	Calcite	Dolomite	Anhydrite	Halite	Albite	Kaolinite	Ca–Mg/Na Ex	CH_2O	$CO_2(g)$
A	60	30	−1.70	0.04	0.96	1.22	1.16	−1.72			−0.79
A	69	78	0.18	−0.07	0.02	0.03		0.00	−0.12		−1.16
B	81	37	−2.29	0.61	1.30	5.18		−0.03	1.45		−3.31
B	81	43	−0.60	−0.09	0.12	0.35		−0.03	0.23		−3.67
C	130	124	0.12	0.45		10.08	0.21	−0.27		1.33	
C	132	130	−0.87	0.24			2.08	−3.11		2.44	
D	115	90	−7.91	3.70	5.06		1.93	−2.89		2.15	
E	118	106	−1.20	0.24	0.07		2.53	−3.87		1.52	
E	118	107	−1.57	0.66		0.12	1.69	−2.65		2.76	

*Postive values, dissolution.
*Negative values, precipitation.

Table 4
Radiometric ages of groundwaters

ID#	Measured $a^{14}C$ (pmc)[a]	Unadjusted age (years)	Calculated age Tamers (1975)	Calculated age Pearson and Hanshaw (1970)	Calculated age Fontes and Garnier (1979)	Calculated age mass balance NETPATH
37	4.39	25,840	20,190	13,700	17,390	20,656
43	3.14	28,610	23,060	12,010	17,180	23,500
30	5.76	23,600	18,160	12,110	14,810	18,466
78	42.26	7120	1580	330	370	486
90	42.11	7150	2140	3210	2560	2802
92	74.3[b]	2460	Modern	Modern	Modern	Modern
106	7.56	21,350	15,920	17,620	17,160	17,298
107	0.12	55,600	50,430	50,180	50,400	50,371
124	4.14[c]	26,330	14,320	13,870	13,950	14,135
130	4.60	25,460	19,780	12,570	16,020	16,217

[a] Percent modern carbon.
[b] Carbon-14 analysis from Eberts and George (2000).
[c] Additional corrections made for microbial activity—see text for discussion.

Michigan Basin and northern margin of the Illinois Basin have elevated Br^-, Na^+, and Cl^- concentrations from mixing with NaCaClBr-rich basinal brines. The majority of groundwaters have higher Na^+/Cl^- ratios than basinal brines and halite, indicating additional Na^+ may have been provided by cation exchange reactions with clays.

4.4. Carbonate mineral dissolution

The majority of groundwaters in glacial drift and underlying Devonian carbonate aquifers, along the basin margins, are $CaMgHCO_3$ waters. These fluids have $Ca^{2+} + Mg^{2+}$ versus alkalinity molar ratios of 1:2 (Fig. 8a) indicative of carbonate mineral dissolution, according to the stoichiometry of the following reactions:

$$CaCO_3 + CO_2 + H_2O = Ca^{2+} + 2HCO_3^- \quad (1)$$

$$CaMg(CO_3)_2 + 2CO_2 + 2H_2O = Ca^{2+} + Mg^{2+} + 4HCO_3^- \quad (2)$$

Several groundwaters have compositions, which fall below the line for calcite and dolomite dissolution, depleted in Ca^{2+} and Mg^{2+}, relative to HCO_3^-, and enriched in Na^+. These $NaHCO_3$ waters are located downgradient in discharge areas confined by lake-bed clays. Mass and charge balance calculations show that the deficits in $Ca^{2+} + Mg^{2+}$ can be accounted for by significant additions of Na^+ above that contributed from NaCl dissolution, demonstrating these $NaHCO_3$ waters likely evolved from ion exchange reactions with clays (Hendry and Wassenaar, 2000).

Several of the groundwaters have elevated Ca^{2+} and Mg^{2+} concentrations relative to HCO_3^-, and are charge balanced by SO_4^{2-}. These sulfate-rich waters likely evolved from anhydrite ($CaSO_4$) dissolution in confined portions of the regional aquifer system, or by pyrite oxidation (FeS_2) in recharge areas. Although the majority of groundwaters are saturated with respect to calcite and dolomite, they remain undersaturated with respect to gypsum/anhydrite. Dissolution of anhydrite by dilute waters at depth in evaporite-bearing carbonate units increases the Ca^{2+} and SO_4^{2-} concentrations:

$$CaSO_4 = Ca^{2+} + SO_4^{2-} \quad (3)$$

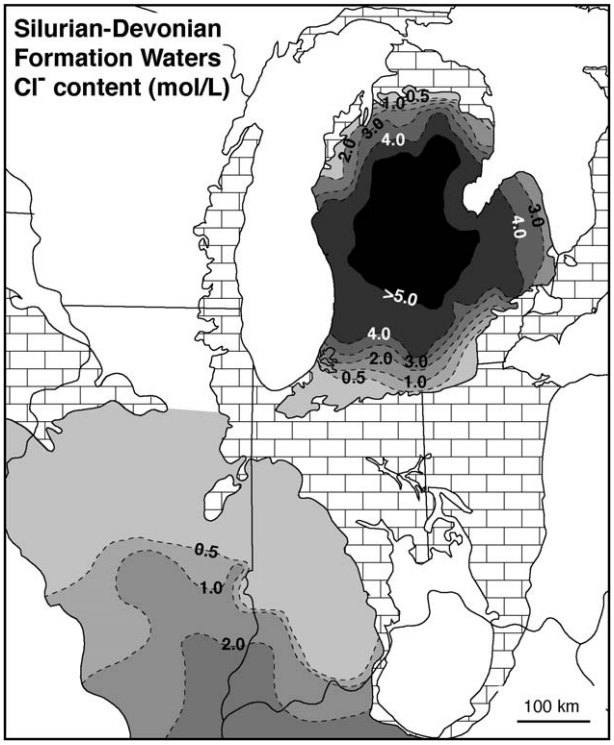

Fig. 4. Salinity structure of fluids in Silurian-Devonian carbonate aquifers in the Illinois and Michigan basins superimposed on the carbonate subcrop.

As the Ca^{2+} concentration increases in the water, the common ion effect may cause calcite supersaturation and precipitation, decreasing Ca^{2+} and HCO_3^- concentrations. The decrease in HCO_3^- concentrations may then cause dolomite to become undersaturated and dissolve, adding Mg^{2+} to the waters and decreasing the Ca/Mg molar ratios. The net reaction for this geochemical process is:

$$CaMg(CO_3)_2 + CaSO_4 + H^+ = CaCO_3 + Ca^{2+} + Mg^{2+} + SO_4^{2-} + HCO_3^- \quad (4)$$

Pyrite oxidation and subsequent carbonate mineral dissolution produces the same products as the above reaction:

$$FeS_2 + 3.75O_2 + 3.5H_2O = Fe(OH)_3 + 2H_2SO_4 \quad (5)$$

$$CaMg(CO_3)_2 + H_2SO_4 = Ca^{2+} + Mg^{2+} + SO_4^{2-} + 2HCO_3^- \quad (6)$$

Sulfate-rich groundwaters affected by dedolomitization plot along the 1:1 $Ca^{2+} + Mg^{2+}$ versus $SO_4^{2-} + 0.5HCO_3^-$ line in Fig. 8b. Sulfur and oxygen isotope chemistry of the dissolved sulfate is the most reliable geochemical tracer for distinguishing between pyrite oxidation and sulfate reduction.

Three of the NaCl groundwaters have elevated $Ca^{2+} + Mg^{2+}$ concentrations relative to carbonate mineral dissolution from mixing with basinal brines, rather than from anhydrite dissolution or pyrite oxidation. Several of the NaCl and $NaHCO_3$ waters plot below the lines for carbonate mineral dissolution and dedolomitization reaction stoichiometries. These fluids are likely enriched in HCO_3^- from sulfate reduction and/or methanogenesis, and enriched in Na^+ from mixing with basinal brines and/or cation exchange with clays. Carbon isotope values of the dissolved inorganic carbon (DIC), together with sulfur isotope chemistry can help elucidate the major biogeochemical processes.

The mass-balance modeling program NETPATH (Plummer et al., 1994) was used to quantify the principal processes controlling the geochemical evolution of groundwaters, identified above: dissolution of calcite, dolomite, anhydrite, and halite; precipitation of calcite; cation exchange with clays ($Ca^{2+} + Mg^{2+}/Na^+$); and oxidation

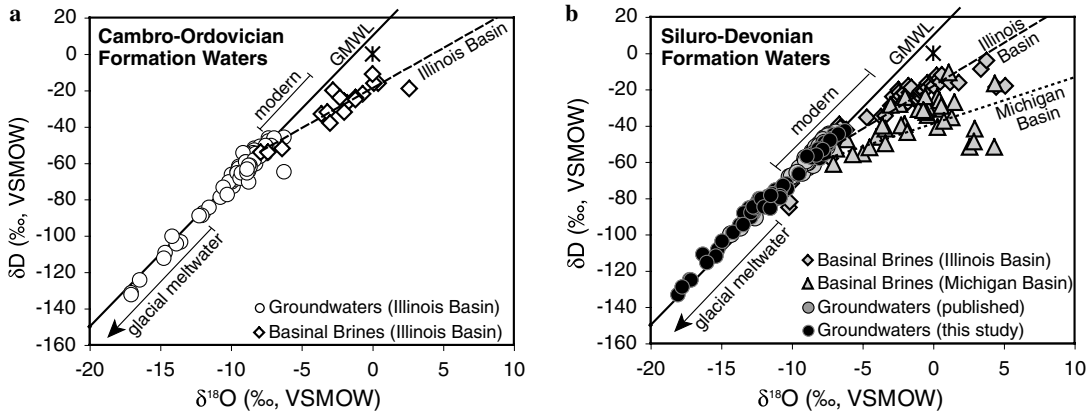

Fig. 5. Source of meteoric waters in the Illinois and Michigan basin regional aquifer systems. (a) Oxygen and hydrogen isotope composition of waters in Cambrian-Ordovician aquifers in the Illinois Basin (Siegel and Mandle, 1984; Siegel, 1991; Stueber and Walter, 1994), overlain on the Global Meteoric Water Line (GMWL; Craig (1961)). Illinois basinal brines fall along a trajectory to the right of the GMWL, represented by the dotted trendline. The standard mean ocean water value (SMOW) is shown in the asterisk. Modern precipitation $\delta^{18}O$ values range from −7.5 to −4.5‰ in the Illinois Basin. Estimated $\delta^{18}O$ values for glacial meltwater in the Great Lakes region range from −25 to −11‰ (see text for references). (b) Formation waters in Silurian-Devonian aquifers in the Illinois and Michigan basins. Black filled circles represent new groundwater data from this study, compared to previously published Silurian-Devonian groundwaters (shown in grey circles) (Nicholas et al., 1996; Eberts and George, 2000; Ku, 2001). Brines in Illinois and Michigan basin Silurian-Devonian strata are also shown for reference (Clayton et al., 1966; Stueber and Walter, 1991; Wilson and Long, 1993a,b; McIntosh et al., 2002). The $\delta^{18}O$ values of modern precipitation in the Illinois and Michigan basins range from −11.0 to −4.5‰.

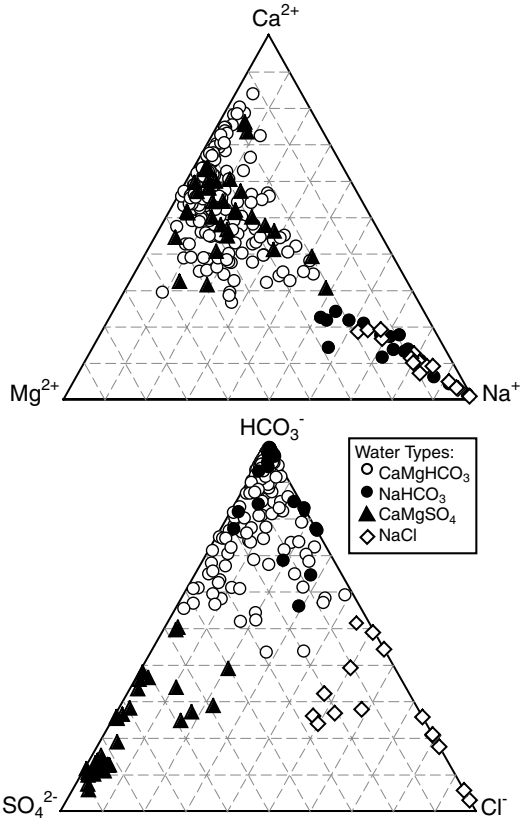

Fig. 6. Ternary diagrams showing major cation and anion chemistry (in equivalents) of groundwaters in Silurian-Devonian carbonate and glacial drift aquifers. Fluids are divided into four geochemically distinct groups: $CaMgHCO_3$-, $CaMgSO_4$-, $NaHCO_3$-, and NaCl-type waters. The four subgroups and symbols are used in the following figures.

of organic matter. It was also assumed that dissolution of aluminosilicate minerals, such as albite in the glacial drift, and back precipitation of kaolinite were important for the silica and Na^+ budgets. Net geochemical reactions were modeled for a subset of groundwaters along several inferred flow paths (transects shown in Fig. 3); initial and final wells were chosen based on hydraulic gradients and chemical composition (Table 3). As predicted, dolomite, anhydrite, and halite dissolution are important contributors of Ca^{2+}, Mg^{2+}, SO_4^{2-}, Na^+, and Cl^- to the aquifers. Sodium was also added by dissolution of silicate minerals and cation exchange with clays. Calcite was dissolved and back precipitated along seven of the nine flow paths. Microbial processes, such as sulfate reduction and methanogenesis likely oxidized organic matter in the aquifers, and consumed CO_2. CO_2 could also have been consumed by dissolution of carbonate minerals. Large quantities of halite dissolved along flow paths across the northern and southern margins of the Michigan Basin, where Silurian-Devonian carbonate aquifers contain localized and bedded evaporites. Na^+ and Cl^- were also added to groundwaters along the southern basin margin through mixing with brines.

4.5. Ca^{2+}–Mg^{2+} relations and carbonate mineral saturation states

Shallow glacial drift waters have Ca^{2+}/Mg^{2+} molar ratios of ~2, indicating congruent dissolution of equal proportions of calcite and dolomite (Szramek and Walter, 2004). Groundwaters in deep glacial drift and Silurian-Devonian aquifers have variable Ca^{2+}/Mg^{2+} ratios, most ranging from 2:1 to 1:1, reflecting the multiple geochemical processes affecting the waters, such as anhydrite dissolution and incongruent dissolution of carbonate minerals (Fig. 9a). Selective leaching of Mg^{2+} and Sr^{2+} from freshly ground surface layers of calcite minerals, for example during glaciation, may have also lowered the Ca^{2+}/Mg^{2+} and Ca^{2+}/Sr^{2+} ratios in solution (McGillen and Fairchild, 2005).

As observed in Fig. 8, $CaMgSO_4$ groundwaters have the highest Ca^{2+} and Mg^{2+} concentrations, with variable Ca^{2+}/Mg^{2+} ratios. NaCl and $NaHCO_3$ groundwaters have relatively low Ca^{2+} and Mg^{2+} concentrations. The majority of Silurian-Devonian carbonate groundwaters and glacial drift waters are saturated to supersaturated with respect to calcite, and at saturation with respect to dolomite (Fig. 9b). A few $NaHCO_3$ and $CaMgHCO_3$ waters are undersaturated with respect to dolomite; these dilute waters are located in recharge areas of the glacial drift and bedrock aquifers. All of the $CaMgSO_4$ waters are supersaturated with respect to calcite, further evidence of the common ion effect of Ca^{2+} from anhydrite dissolution.

4.6. Strontium isotope chemistry: Sources of Sr^{2+}

Incongruent dissolution of calcite and dolomite, and dissolution of anhydrite, enriches the fluids in both Sr^{2+} and Mg^{2+}. As the Sr^{2+} concentration increases, the Ca^{2+}/Mg^{2+} ratio of groundwaters decreases, suggesting progressive water–rock interactions (shown in Fig. 10a). A few of the $CaMgHCO_3$ groundwaters in shallow glacial drift aquifers have high Ca^{2+}/Mg^{2+} ratios (>2) and low Sr^{2+} concentrations, indicating they likely dissolved more calcite than dolomite. $CaMgSO_4$ waters have elevated Sr^{2+} concentrations relative to the majority of $CaMgHCO_3$ waters. Evaporite dissolution may enrich fluids in Sr^{2+}, as evaporite minerals, such as celestite, contain more Sr^{2+} than calcite and dolomite. Jacobson and Wasserburg (2005) show that anhydrite dissolution in the Madison carbonate aquifer system in western South Dakota contributes the vast majority of Sr^{2+} to the groundwater. Divalent cation relations (e.g., Ca^{2+}/Mg^{2+}, Sr^{2+}/Ca^{2+}, and Sr^{2+}/Mg^{2+}) are dependent on the molar ratios of the minerals dissolved and precipitated in the aquifer and by adsorption onto clays (Banner, 1995). Mixing of meteoric waters with basinal brines may also increase Sr^{2+} concentrations, as shown by the NaCl waters with high Sr^{2+}values (>50 μm). Divalent cation ratios may be used as qualitative age indicators, as fluids with higher Mg^{2+}/Ca^{2+} and Sr^{2+}/Ca^{2+} ratios likely have longer residence times (Kloppmann et al.,

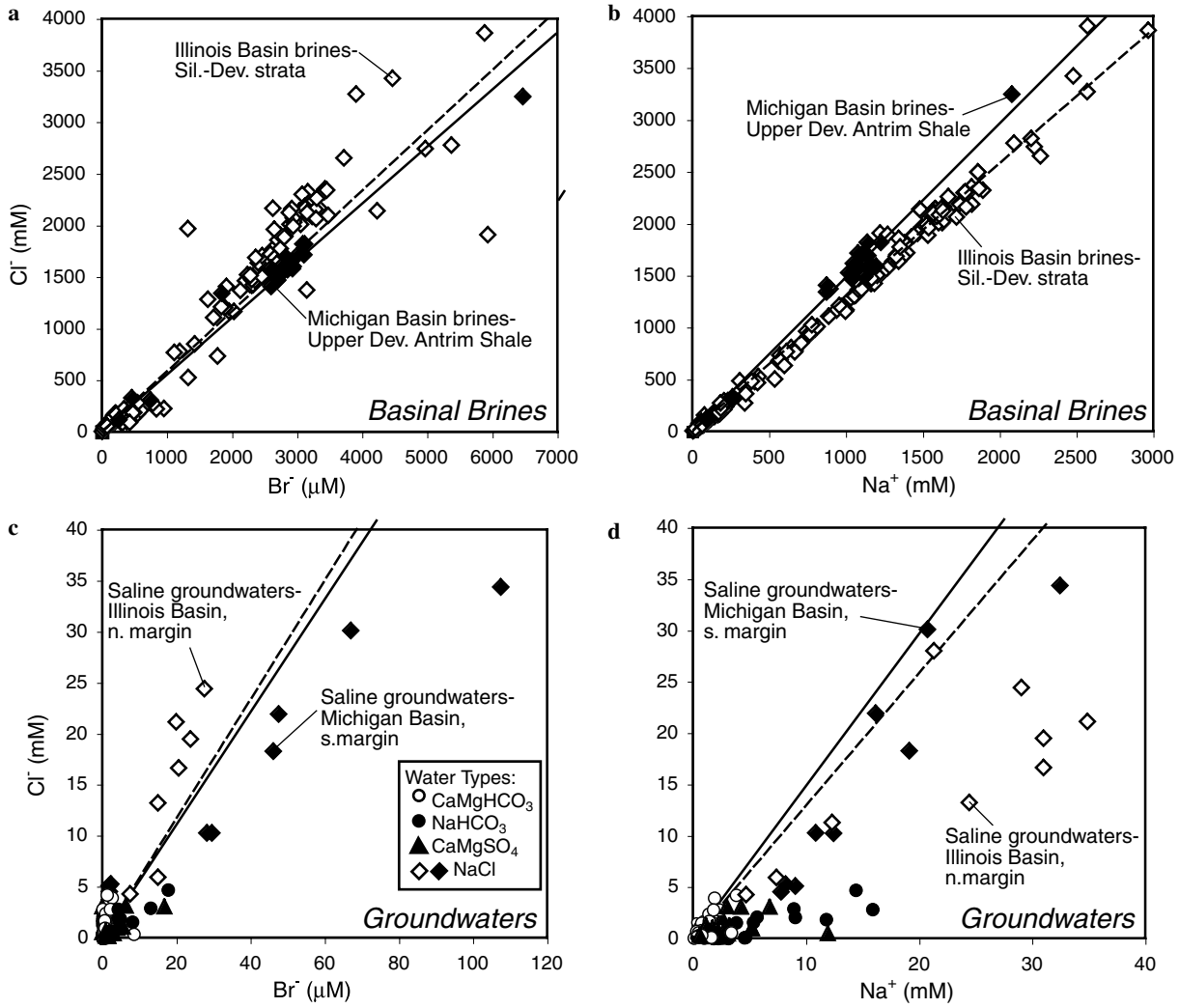

Fig. 7. Cl–Br–Na relations and sources of salinity in Silurian-Devonian carbonate aquifers in the Michigan and Illinois basins. (a) Cl–Br concentrations of Silurian-Devonian brines in the Illinois Basin, shown in open diamonds, and Devonian Antrim Shale brines, along the southern margin of the Michigan Basin, shown in closed diamonds (Stueber and Walter, 1991; McIntosh et al., 2002, 2004). Trendlines represent mixing of meteoric waters (with no Cl^- and Br^-) with these NaClBr-rich saline fluids. (b) Cl–Na relations of basinal formation waters, also showing mixing of dilute waters with saline brines. (c and d) Re-seated view of the Silurian-Devonian carbonate groundwaters, in relation to the basinal brines and mixing trends from above. NaCl-type fluids from the margins of the Illinois Basin are shown in open diamonds, while NaCl-type fluids from the southern margin of the Michigan Basin are shown in closed diamonds. NaCl-type groundwaters from the northern margin of the Michigan Basin plot near the origin, with relatively low Cl^-, Na^+, and Br^- values.

1998; Elliot et al., 1999; Musgrove and Banner, 2004; Szramek et al., 2004).

The major sources of Sr^{2+} in the Silurian-Devonian regional aquifer system are carbonate mineral and anhydrite dissolution, mixing with basinal brines, cation exchange with radiogenic clays and shales, and dissolution of silicate minerals in overlying glacial drift. The strontium isotope composition of groundwaters can be used to trace the sources of Sr^{2+}, water–rock interactions, and fluid mixing, which are especially important for constraining the groundwater ^{14}C ages (Bishop et al., 1994; Lyons et al., 1995; Johnson and DePalo, 1997; Hogan et al., 2000).

In general, Silurian-Devonian carbonates have $^{87}Sr/^{86}Sr$ values similar to Silurian-Devonian seawater, which ranged from 0.7078 to 0.7088, as shown in the grey box in Fig. 10b (Burke et al., 1982; Veizer et al., 1999). Devonian carbonates in the Illinois Basin have $^{87}Sr/^{86}Sr$ ratios of ~0.7083 (Stueber et al., 1987). The $^{87}Sr/^{86}Sr$ values of anhydrite in the Upper Silurian Salina Group, Michigan Basin, range from 0.7086 to 0.7087 (Das et al., 1990), also within the range of Silurian-Devonian seawater.

Michigan Basin brines in Silurian-Devonian carbonates have $^{87}Sr/^{86}Sr$ ratios ranging from 0.7080 to 0.7095 (McNutt et al., 1987; Wilson and Long, 1993a,b), similar to the Silurian-Devonian seawater values. Brines in Illinois Basin Silurian-Devonian carbonates, on the other hand, have more radiogenic Sr isotope values (0.7092–0.7108), indicating a significant portion of the Sr^{2+} came from interactions with the overlying radiogenic Upper Devonian

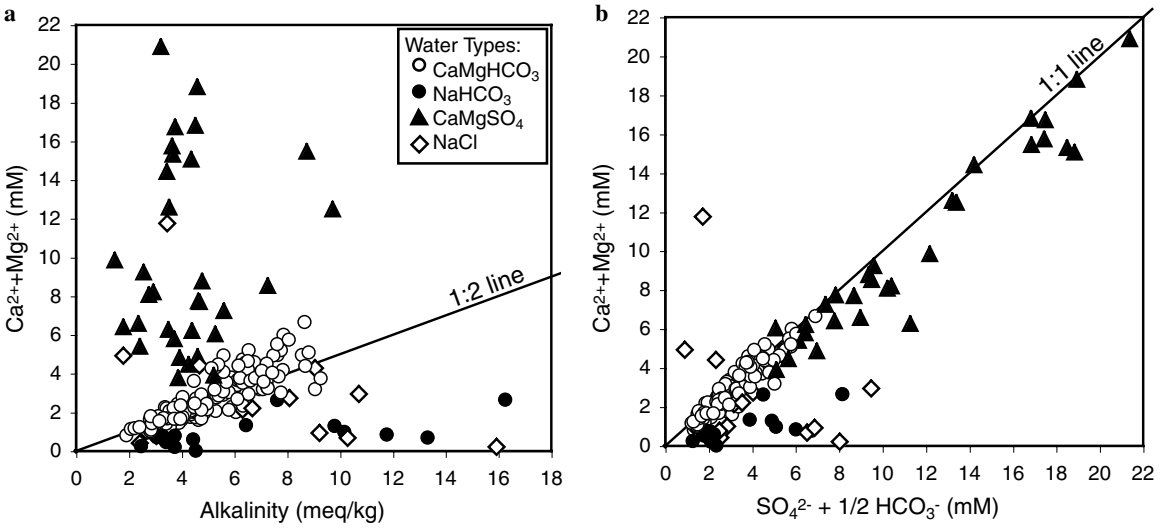

Fig. 8. Carbonate mineral dissolution and dedolomitization. (a) $Ca^{2+} + Mg^{2+}$ versus alkalinity concentrations for groundwaters in Silurian-Devonian carbonate and glacial drift aquifers. $CaMgHCO_3$-type waters plot along the 1:2 line for $Ca^{2+} + Mg^{2+}$ versus alkalinity, indicating they likely evolved from carbonate mineral dissolution. (b) Fluids enriched in $Ca^{2+} + Mg^{2+}$ and SO_4^{2-} fall along the 1:1 line for dedolomitization.

shale (Stueber et al., 1987; Stueber and Walter, 1991). The similar Sr isotope compositions of Michigan Basin Silurian-Devonian brines and carbonate bedrock (Fig. 10b) make it difficult to distinguish between the Sr^{2+} derived from mixing with basinal brines and that derived from interactions with carbonate minerals.

The majority of groundwaters have $^{87}Sr/^{86}Sr$ values within the range of the carbonate and anhydrite in the Silurian-Devonian bedrock (Fig. 10b), indicating the fluids are buffered by water–rock interactions with the aquifer matrix. Groundwaters with high Sr^{2+}/Ca^{2+} ratios have been extensively altered by incongruent dissolution of carbonate minerals and dissolution of anhydrite. Several of the groundwaters plot just above the range for Silurian-Devonian seawater Sr isotope values. These fluids have also likely evolved from water–rock interactions with carbonate and anhydrite, and may have some Sr^{2+} contributed from dissolution of more radiogenic silicate minerals or cation exchange reactions with clays or Upper Devonian shales ($^{87}Sr/^{86}Sr = 0.7102$–0.7129, Stueber et al. (1987)). Elevated $^{87}Sr/^{86}Sr$ values (>0.7100) of several $CaMgHCO_3$ waters, with low Sr^{2+}/Ca^{2+} ratios, likely reflect dissolution of silicate minerals in shallow glacial drift aquifers. Strontium isotope ratios were not analyzed in the RASA study (Eberts and George, 2000) or the US Geological Survey groundwater study in southeastern Michigan (Nicholas et al., 1996).

4.7. Sulfur and oxygen isotope chemistry: Sources of SO_4^{2-}

Discriminating between pyrite oxidation and gypsum dissolution is important for constraining the origin of solutes and migration pathways for fluids along the basin margins (Dogramaci et al., 2001). Geochemical processes such as pyrite oxidation and/or sulfate reduction may also affect carbon isotope systematics, which are used in calculating radiocarbon ages of groundwater. Sulfur and oxygen isotope values of SO_4^{2-}, in tandem with Sr isotope geochemistry, can help to distinguish between the major sources of SO_4^{2-}, Ca^{2+}, and Sr^{2+}.

The $CaMgSO_4$ groundwaters all have high SO_4^{2-} concentrations and variable $\delta^{34}S$ values for SO_4^{2-}, shown in Fig. 11a. As previously discussed, these fluids likely became enriched in SO_4^{2-} via pyrite oxidation or anhydrite dissolution. Sulfur isotope values of anhydrite in evaporite-bearing Silurian-Devonian carbonates in the Michigan Basin range from +24.9 to +28.7‰ (Das et al., 1990; Eberts and George, 2000), while $\delta^{34}S$ values of Silurian-Devonian seawater range from approximately +17 to +30‰ (Claypool et al., 1980). Several groundwater samples have $\delta^{34}S$ values consistent with anhydrite dissolution. These fluids are located in confined aquifers along the southeastern and northern margins of the Michigan Basin. Although the groundwaters are undersaturated with respect to gypsum, the saturation indices for gypsum approach zero (saturation) with increasing SO_4^{2-} concentration. Groundwaters in confined Cambrian-Ordovician aquifers along the northern margin of the Illinois Basin also show evidence for anhydrite dissolution (Gilkeson et al., 1981). Siegel (1990) suggested that Pleistocene glacial meltwaters dissolved anhydrite in Silurian carbonates beneath the lobe of the Lake Michigan Ice Sheet and migrated into the underlying evaporite-poor Cambrian-Ordovician aquifers in the Illinois Basin.

The $\delta^{34}S$ values of sedimentary sulfides typically range from −50 to +10‰ (Karim and Veizer, 2000). Secondary gypsum deposits in glacial drift have $\delta^{34}S$ values within the range of sulfide minerals, from −14.8 to −8.2‰ (Eberts and George, 2000). Several groundwaters have $\delta^{34}S$ values within the range of pyrite oxidation and secondary gyp-

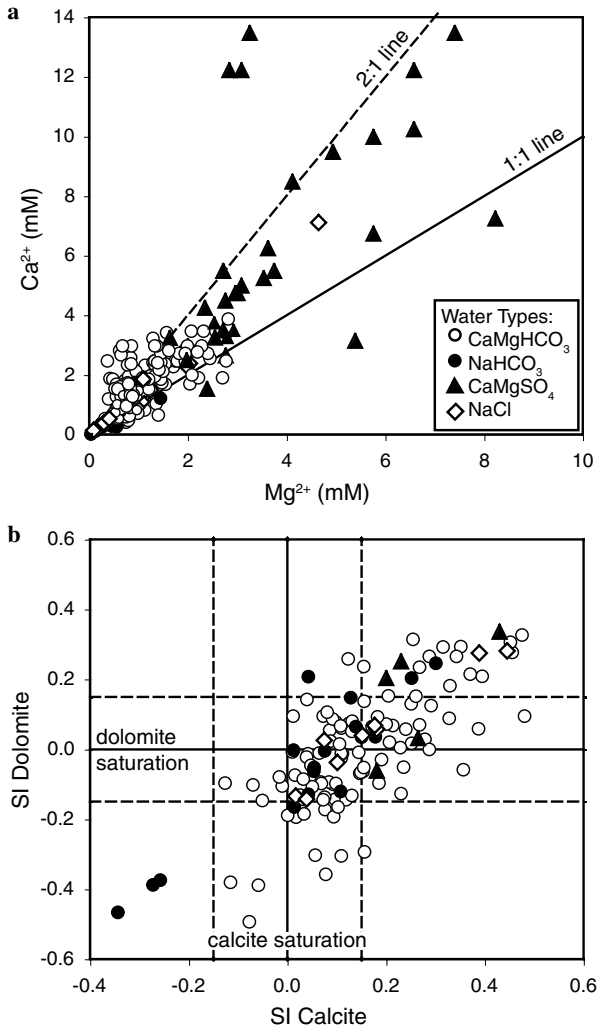

Fig. 9. Ca^{2+}–Mg^{2+} relations and carbonate mineral saturation states. (a) Ca^{2+} and Mg^{2+} concentrations of groundwaters in Silurian-Devonian carbonate and glacial drift aquifers. The 2:1 and 1:1 lines for Ca^{2+}:Mg^{2+} ratios are shown for reference. (b) Saturation indices [SI = Log(IAP/K)] for calcite and poorly ordered dolomite, calculated from SOLMINEQ.88 (Kharaka et al., 1988) and Hyeong and Capuano (2001)—see Section 3 for a detailed discussion of mineral saturation state modeling. Groundwaters with SI values between −0.15 and 0.15 are considered to be at equilibrium with calcite and/or poorly ordered dolomite.

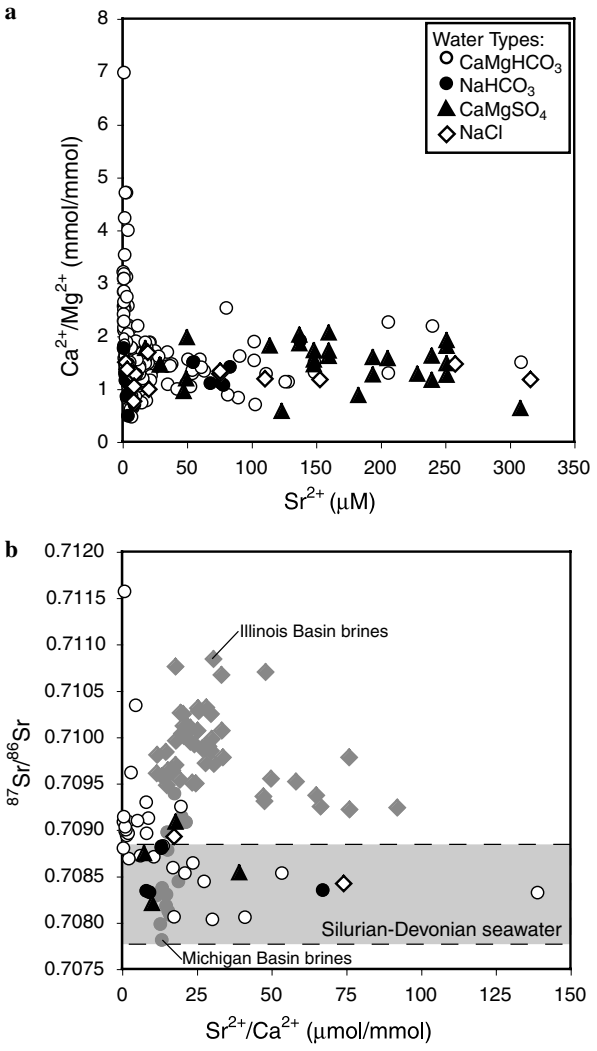

Fig. 10. Ca–Mg–Sr relations of groundwaters in Silurian-Devonian carbonate and glacial drift aquifers. (a) Ca^{2+}/Mg^{2+} ratios versus Sr^{2+} concentration. (b) Strontium isotope ratios versus Sr^{2+}/Ca^{2+} molar ratios. The range of strontium isotope values of Silurian and Devonian seawater are shown for reference in the grey box (Burke et al., 1982; Veizer et al., 1999). Saline waters in Silurian-Devonian aquifers from the Illinois and Michigan basin are also shown for comparison. Michigan Basin brines (Wilson and Long, 1993a,b) are shown in grey filled circles and Illinois Basin brines (Stueber and Walter, 1991) are shown in grey filled diamonds.

sum, indicating these fluids became enriched in SO_4^{2-} in unconfined portions of the aquifer system. The majority of these groundwaters are from the RASA study, in recharge areas of the Silurian-Devonian carbonate subcrop and overlying glacial drift (Eberts and George, 2000).

A few of the groundwater samples had exceptionally high $\delta^{34}S$ values (>+30‰), indicative of isotope fractionation associated with microbial sulfate reduction. Several of the groundwaters also had low to no SO_4^{2-}, together with detectable H_2S concentrations, confirming the importance of sulfate reduction in confined areas of the regional aquifers. Microbial sulfate reduction produces carbonate alkalinity (refer to Fig. 8), which can cause calcite to become supersaturated:

$$2CH_2O + SO_4^{2-} = H_2S + 2HCO_3^- \quad (7)$$

Microbial sulfate reduction extracts the lighter sulfur (^{32}S) and oxygen (^{16}O) isotopes, enriching the residual fluids in ^{34}S and ^{18}O. Kinetic fractionations of +4 to +46‰ and +4 to +29‰ have been reported for $\delta^{34}S$ and $\delta^{18}O$, respectively, (for references see Ku et al. (1999)), dependent on the environmental conditions and microbial communities present in the flow system. In contrast, sulfur isotope values of SO_4^{2-} in groundwaters affected by sulfide oxidation are usually only marginally depleted from the original sulfide (Clark and Fritz, 1997), and only small $\delta^{18}O$–SO_4 fractionations are observed (0 to +8.7‰) (Ku et al., 1999) (Fig. 11b). Oxygen isotope compositions from both

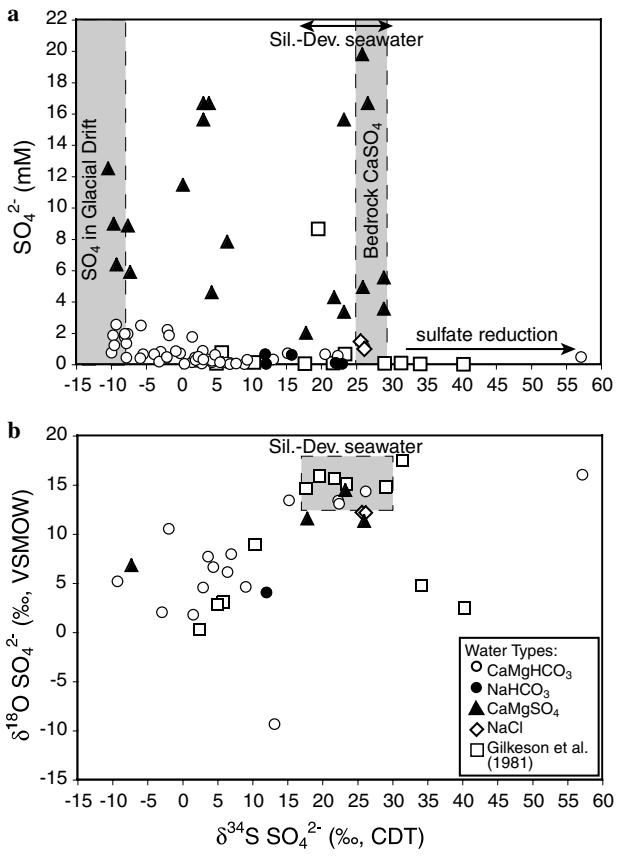

Fig. 11. Sulfur and oxygen isotope composition of dissolved sulfate in groundwaters in Silurian-Devonian carbonate and glacial drift aquifers. (a) $\delta^{34}S$ values of SO_4^{2-} versus SO_4^{2-} concentration. The $\delta^{34}S$ value of gypsum and anhydrite in Silurian-Devonian bedrock in the study area ranged from 24.9 to 28.7‰, whereas the $\delta^{34}S$ value of secondary gypsum in glacial drift deposits ranged from −14.8 to −8.2‰ (Eberts and George, 2000). (b) Oxygen isotope composition versus $\delta^{34}S$ value of SO_4. Groundwaters in Cambrian-Ordovician aquifers, along the northern margin of the Illinois Basin, are shown for comparison (Gilkeson et al., 1981). The $\delta^{34}S$ and $\delta^{18}O$ values of Silurian-Devonian seawater are shown for reference (Claypool et al., 1980).

the atmosphere (+23.5‰) and water (−17 to −6‰) can influence the $\delta^{18}O$ value of SO_4 during pyrite oxidation, possibly explaining the low $\delta^{18}O$–SO_4 value (−9.3‰) of one of the groundwater samples (Sidle, 2002). In contrast, anhydrite dissolution does not alter the $\delta^{34}S$ value of the SO_4^{2-} and exchange of $\delta^{18}O$ in SO_4^{2-} and H_2O is relatively slow; both the $\delta^{18}O$ and $\delta^{34}S$ values of the groundwaters likely resemble the evaporite minerals being dissolved (Clark and Fritz, 1997) (Fig. 11b).

4.8. Carbon isotope systematics

Carbon system parameters and $\delta^{13}C$ values of dissolved inorganic carbon (DIC) are important in determining the sources of carbon and tracing water–rock and microbial interactions. Within the observed pH and PCO_2 range of groundwaters in glacial drift and Silurian-Devonian carbonate aquifers, the DIC is equivalent to the alkalinity. Soil gases (CO_2) in northern Michigan have average $\delta^{13}C$ values of −21.9‰ (Ku, 2001). Carbonate minerals in the glacial drift and bedrock have $\delta^{13}C$ values ranging from −4.1 to +0.5‰, within the range of Paleozoic carbonates (Ku, 2001; Budai et al., 2002). Congruent dissolution of carbonate minerals with soil CO_2 would produce $\delta^{13}C_{DIC}$ values of approximately −12.5 and −11.1‰ under open versus closed system conditions, respectively. Ku (2001) reported that shallow glacial drift waters in northern Michigan had $\delta^{13}C_{DIC}$ values of −12.2‰ on average. Soil waters in southern Indiana, overlying epikarst, have slightly lower $\delta^{13}C$ values for DIC (−14.7‰) (Yu and Krothe, 1997) (Fig. 12a).

Groundwaters in the recharge areas with relatively permeable glacial drift have carbon isotope values consistent with open system carbonate mineral dissolution. These are predominately $CaMgHCO_3$ waters (Fig. 12a). Fluids with lower alkalinity values (<4.5 meq/kg), high $\delta^{13}C$ values of DIC (−10 to 0‰), and enriched Mg^{2+} and Sr^{2+} concentrations likely evolved via incongruent dissolution of carbonate minerals under closed system conditions. Several of the $CaMgSO_4$, $NaHCO_3$, and NaCl waters also have high $\delta^{13}C$ and low alkalinity values, and depleted Ca^{2+}/Mg^{2+} and Ca^{2+}/Sr^{2+} ratios, reflecting their isolation from active shallow groundwater flow systems and longer residence times. Carbonate dissolution likely occurs first under open system conditions in the recharge areas, near the water table, and then under closed system conditions in the discharge areas and along the regional groundwater flow paths.

Groundwaters with $\delta^{13}C$ values for DIC greater than +15‰ have been significantly affected by microbial methanogenesis in Upper Devonian black shales (Martini et al., 1998). These fluids are located along the southeastern margin of the Michigan Basin adjacent to known Antrim Shale microbial gas deposits. Higher alkalinity values (>10 meq/kg) were likely generated by microbial methanogenesis, as observed in Antrim Shale formation waters, and have been lowered by subsequent calcite precipitation (McIntosh et al., 2004).

As shown in the sulfur isotope chemistry, sulfate reduction is also a significant microbial process that has altered the carbon system. Like methanogenesis, sulfate reduction increases the alkalinity, however during sulfate reduction the $\delta^{13}C$ value of DIC becomes more negative. The Silurian-Devonian carbonate groundwater with the anomalously high $\delta^{34}S$ value for SO_4^{2-} (+57.07‰) has a low $\delta^{13}C$ value for DIC (−20.44‰), consistent with sulfate reduction. Several other groundwater samples with low $\delta^{13}C$ values for DIC (<−15‰) may have also been affected by sulfate reduction.

It is critical to understand the major sources and sinks for carbon in the groundwater flow systems to use carbon isotopes of DIC to estimate groundwater ages (Kloppmann et al., 1998). A plot of the activity of ^{14}C (in percent modern carbon) versus the $\delta^{13}C$ value of DIC illustrates the main geochemical processes affecting the carbon isotope

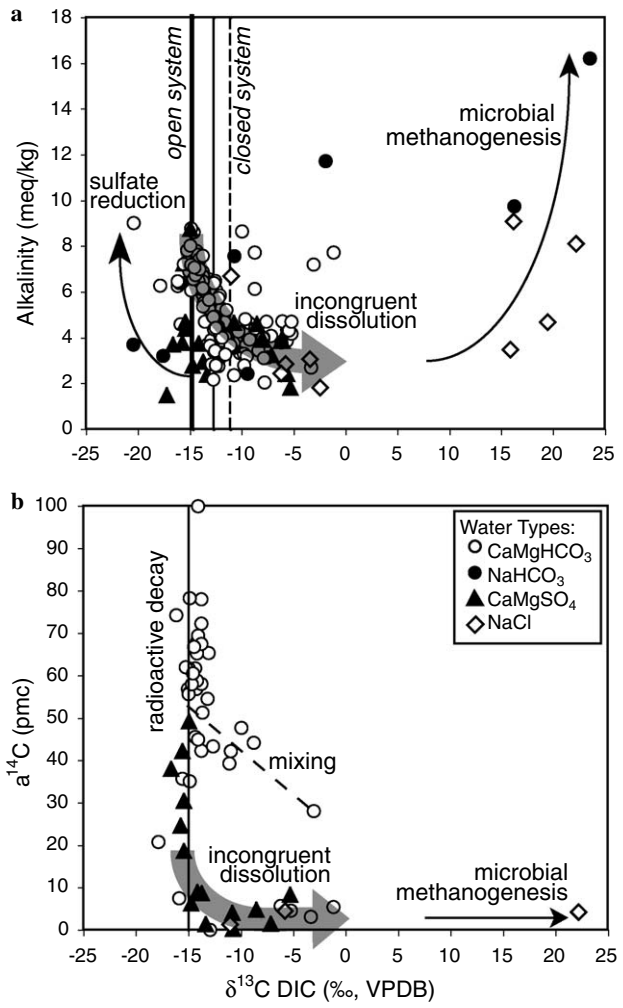

Fig. 12. Carbon isotope composition of dissolved inorganic carbon (DIC). (a) Alkalinity versus $\delta^{13}C$ DIC values of groundwaters in Silurian-Devonian and glacial drift aquifers. $\delta^{13}C$ values of DIC in soil waters in northern Michigan range from −12.5‰ to −11.1‰ for open and closed system conditions, respectively (Ku, 2001). Soil waters overlying epikarst in Indiana have average $\delta^{13}C_{DIC}$ values of −14.7‰ (Yu and Krothe, 1997). (b) Activity of ^{14}C, expressed as percent modern carbon (pmc), versus $\delta^{13}C$ values of DIC.

system (Fig. 12b). Samples selected for carbon-14 analysis all had tritium levels below the detection limit (<0.8 tritium units) indicating they were recharged prior to 1952 (Clark and Fritz, 1997). A few shallow groundwater wells in recharge areas had detectable tritium (Table 2).

The majority of groundwaters with carbon-14 values greater than 10 pmc have $\delta^{13}C$ values similar to those expected for carbonate mineral dissolution under open and/or closed system conditions, with relatively little water–rock reactions. $CaMgHCO_3$ groundwaters with high carbon-14 values (>30 pmc) and more negative $\delta^{13}C_{DIC}$ values (<−14‰) are located in recharge areas of the carbonate aquifers in northern Indiana and Ohio (from Eberts and George (2000) study), where the karstic groundwaters may contain more modern carbon than would be expected by a stoichiometric 1:1 dissolution reaction of carbonates and H_2CO_3. The relative age of these waters can be calculated assuming the decrease in the activity of ^{14}C is primarily due to radioactive decay:

$$t = -8267 \times \ln \frac{a^{14}C_{DIC}}{a_o{}^{14}C},$$

where t is the estimated radiocarbon age (years BP), $a^{14}C_{DIC}$ is the measured activity of ^{14}C in the groundwater sample, and $a_o{}^{14}C$ is the activity of ^{14}C in the soil zone during recharge. Groundwaters with low carbon-14 values (<10 pmc) (Fig. 12b) have been extensively altered by incongruent dissolution of carbonate minerals, which increases the $\delta^{13}C$ value for DIC and decreases the $a^{14}C$, because of the addition of "dead carbon", and significantly increases the apparent age of the groundwaters (Plummer et al., 1990). To correct for the dilution of $a_o{}^{14}C$ through water–rock reactions, several different mixing and mass-balance models were employed (Pearson and Hanshaw, 1970; Tamers, 1975; Fontes and Garnier, 1979; Plummer et al., 1994). The following assumptions were made in the models: $\delta^{13}C_{CO_2} = -25‰$, $\delta^{13}C_{carbonates} = 0‰$, $a^{14}C_{CO_2} = 100‰$, and $a^{14}C_{carbonates} = 0‰$. Table 4 compares the calculated radiocarbon ages of groundwaters using the various methods.

The NaCl-type groundwater sample with a high $\delta^{13}C$ value of DIC (+22‰) also has a low $a^{14}C$ (4.14 pmc), likely because of the addition of "dead carbon" from the oxidation of organic-rich Upper Devonian shales during microbial methanogenesis (Geyh and Kuenzl, 1981) (Fig. 12b, well #124). The $a^{14}C_{DIC}$ for this sample was adjusted to 9.5 pmc, assuming 4.5 meq/kg of alkalinity was added by microbial methanogenesis, following the method of Martini et al. (1998). Several of the groundwaters also appear to have been affected by mixing of fluids with different carbon isotope values.

Regardless of the necessary corrections for carbon sources and sinks, and uncertainties in the calculated ^{14}C "ages," the low $a^{14}C$ for many of the groundwaters and isotopically depleted $\delta^{18}O$ and δD values in confined portions of the regional aquifer system likely indicate these fluids recharged during the Late Pleistocene. Martini et al. (1998) report carbon-14 "ages" of Upper Devonian Antrim Shale formation waters up to 22,000-years-old, along the northern margin of the Michigan Basin. Apparent ^{14}C ages for groundwaters in the RASA study ranged from <50 years BP in recharge areas to >40,000 years BP downgradient in Silurian-Devonian carbonate aquifers beneath lakebed clays near Lake Erie (Eberts and George, 2000). It is notable that radiocarbon ages of confined groundwaters correspond to times when the Silurian-Devonian carbonate subcrop was covered by ice, which is supporting evidence for recharge of meteoric waters beneath the Laurentide Ice Sheet.

4.9. Oxygen and hydrogen isotopes: Source of meteoric waters

Groundwaters in glacial drift and Silurian-Devonian aquifers in the Great Lakes region have $\delta^{18}O$ and δD val-

ues coincident with the meteoric water line, indicating they originated as meteoric recharge (Fig. 13). The vast majority of these groundwaters have stable isotope values significantly lower than modern precipitation. In northern Michigan, NaCl waters are greater than 15,000-years-old and have $\delta^{18}O$ values less than −13‰ (Fig. 13a, Table 4). $CaMgHCO_3$, $NaHCO_3$, and $CaSO_4$ paleowaters also have relatively low $\delta^{18}O$ and δD values. Modern precipitation in this area ranges from −11 to −8‰ $\delta^{18}O$ (IAEA/WMO, 2001; Dutton et al., 2005), whereas Pleistocene-age recharge ranged from approximately −25 to −11‰ (Clayton et al., 1966; McNutt et al., 1987; Long et al., 1988; Dettman et al., 1995; Husain et al., 2004). Two groundwater samples with $\delta^{18}O$ values greater than −8‰ were possibly influenced by mixing with brines.

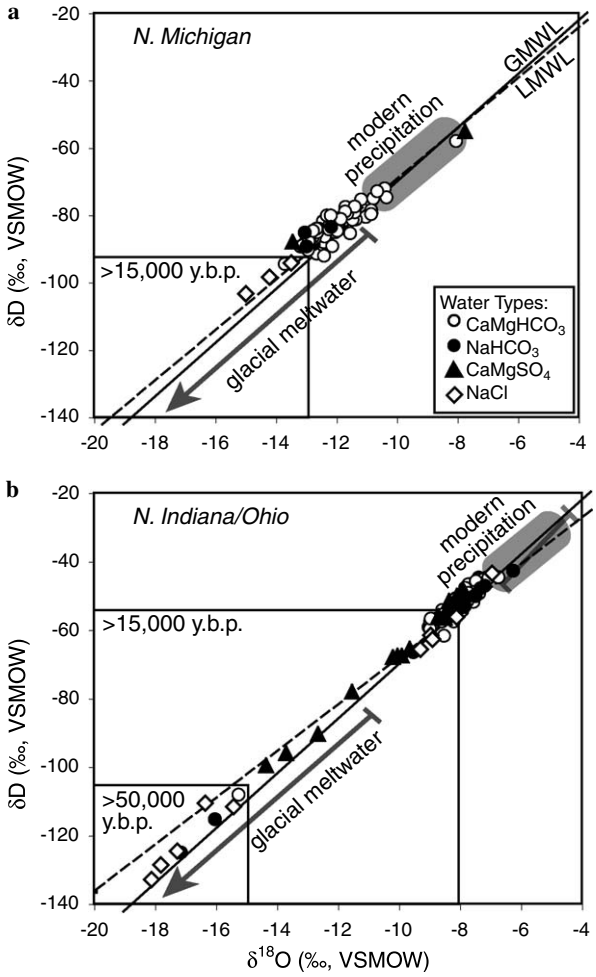

Fig. 13. Oxygen and hydrogen isotope composition of groundwaters in Silurian-Devonian carbonate and glacial drift aquifers in northern Michigan (a), and northern Indiana/Ohio (b), overlain on the Global Meteoric Water Line (GMWL; Craig, 1961). The local meteoric water lines (LMWL) from IAEA stations in close proximity to the study areas, are also shown for reference (IAEA/WMO, 2001). $\delta^{18}O$ values for modern precipitation in northern Michigan range from −11 to −8‰, and from −4.5 to −7‰ in northern Indiana/Ohio. Estimated glacial meltwater $\delta^{18}O$ values range from −25 to −11‰. References for modern and Pleistocene recharge values listed in the text.

Modern recharge in northern Ohio/Indiana ranges from −7 to −4.5‰ (Clayton et al., 1966; Coplen and Kendall, 2000; Eberts and George, 2000; IAEA/WMO, 2001; Dutton et al., 2005). Late-Pleistocene groundwaters in confined aquifers in this region have significantly lower $\delta^{18}O$ and δD values (Fig. 13b), likely from mixing of glacial meltwater and modern precipitation. Consistent with this, the most geochemically evolved groundwaters ($CaSO_4$-, $NaHCO_3$-, NaCl-type) also have the lowest $\delta^{18}O$ and δD values and the longest residence times, as indicated by enriched $\delta^{13}C_{DIC}$, Sr^{2+}, and Mg^{2+} compositions, and depleted carbon-14 values.

5. Summary and implications

Integrating new elemental and isotope analyses of groundwaters in Silurian-Devonian carbonate and overlying glacial drift aquifers, with previously published datasets on groundwaters in recharge areas and deeper basinal fluids, we were able to evaluate the regional extent and geochemical evolution of Pleistocene recharge in confined aquifer systems along the margins of the Illinois and Michigan basins. Modern groundwater flow is primarily restricted to shallow glacial drift aquifers in the Great Lakes region (Fig. 14). During the Pleistocene, however, hydraulic loading of ice sheets reversed regional flow patterns, and focused recharge into Paleozoic aquifers, significantly depressing the freshwater–saline water interface. Dilute waters migrated hundreds of meters into the Silurian-Devonian and Cambrian-Ordovician regional aquifer systems. Radiocarbon ages, and $\delta^{18}O$ and δD values of groundwaters in the Silurian-Devonian carbonates are consistent with recharge beneath the Laurentide Ice Sheets (14–50 ka BP). These paleowaters are isolated from shallow flow systems in overlying glacial drift aquifers. The lowest $\delta^{18}O$ and δD values are found in confined groundwaters beneath relatively impermeable lake-bed clays and tills near the Great Lakes shorelines, and underlying Upper Devonian-Mississippian shales along the Illinois and Michigan basin margins. The presence of isotopically depleted waters in Paleozoic aquifers at relatively shallow depths illustrates the importance of continental glaciation on regional-scale groundwater flow, as these glacial meltwaters have not been flushed by active modern flow systems.

Elemental and isotope geochemistry (O, H, C, S, and Sr) of the confined groundwaters show that they have been extensively altered since the Late Pleistocene by incongruent dissolution of carbonate minerals, dissolution of anhydrite and halite, cation exchange, microbial processes (sulfate reduction and methanogenesis) and mixing with basinal brines. Holocene groundwaters in recharge areas in glacial drift and Silurian-Devonian aquifers have $\delta^{18}O$ and δD values within the range of modern precipitation and are predominately $CaMgHCO_3$ waters, with enriched SO_4^{2-} concentrations from pyrite oxidation. The distinct

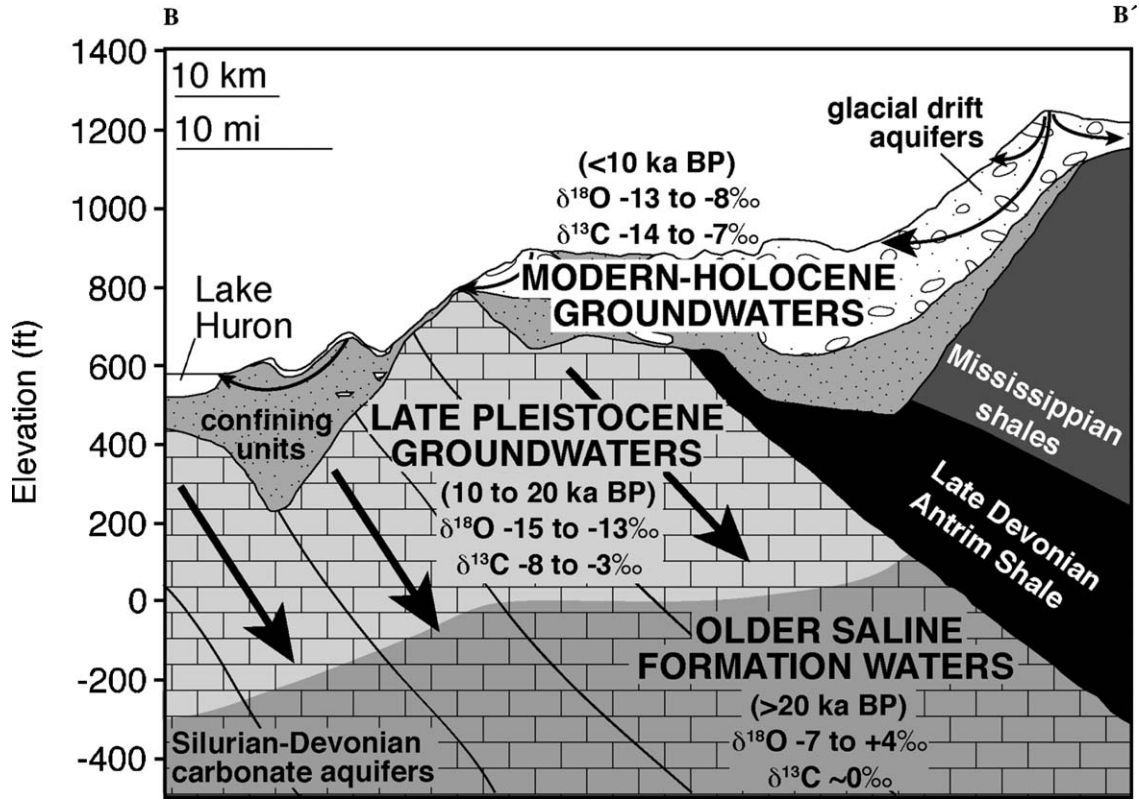

Fig. 14. Schematic diagram summarizing hydrogeology, isotope geochemistry, and relative ages of groundwaters in Silurian-Devonian carbonate aquifers and glacial drift, along the northern margin of the Michigan Basin (cross-section B in Fig. 3). Modern groundwater flow is primarily restricted to shallow drift aquifers (shown in thin arrows). Pleistocene glaciation reversed regional flow patterns (shown in thick arrows) and focused meltwaters down dip into the Michigan Basin, significantly depressing the freshwater–saline water interface. Late Pleistocene waters remain at shallow depths in confined aquifers along the basin margin.

elemental and isotope geochemistry of Pleistocene versus Holocene-age waters further confirms that surficial, topographically driven flow systems are out of contact with the deeper basinal-scale flow systems. Confining units, such as lake-bed clays and shales, are effective barriers to fluid and solute transport in the Great Lakes region. These confining units thus contain archived samples of glacial meltwaters at shallow depths, and are commonly capped microbial methane deposits. The confining units are also important in that they prevent contamination of drinking water resources in underlying aquifers. Hydrologic studies in southwestern Ontario have shown that groundwater flow velocities are less than 0.05 cm/yr within clay-rich tills (Desaulniers et al., 1981). Constraining the impact of Pleistocene glaciation on the hydrogeochemistry of groundwaters in regional aquifers is important for determining the sustainability of potable water resources, water quality and sources of solutes, and response of aquifers to changing climatic conditions.

Acknowledgments

Acknowledgement is made to the donors of the Petroleum Research Fund, administered by the American Chemical Society (PRF Grant 39126, L.M.W.) for partial support of this research. Additional support was provided by the National Science Foundation (NSF-EAR-0208182, L.M.W.). J. C. McIntosh acknowledges support from the Geological Society of America, the American Association of Petroleum Geologists, the Scott Turner Fund and Rackham Graduate School, University of Michigan, and the Morton K. and Jane Blaustein Foundation. We are especially grateful to Demmy Spounias and Heather Whittington for their invaluable help with planning field sampling expeditions, field sampling, lab analyses, and interpretation of the results. We also thank Patti McCall, Naila Moreira, and Larry Jordan Jr. for field sampling assistance. Corey Lambert, Andrea Klaue, Lora Wingate, and Maria Marcano helped with laboratory analyses. We appreciate Anna Martini and Joel Blum's comments on an earlier version of this manuscript. W. Berry Lyons and Alan Stueber generously shared unpublished groundwater data with us for comparison. We thank Ian Fairchild and two other anonymous reviewers for their helpful comments.

Associate editor: Miryam Bar-Matthews

References

Bahr, J. M., Moline, G. R., Nadon, G. C. 1994. Chapter 11: Anomalous pressures in the deep Michigan Basin. In: Ortoleva, P. J. (Ed.), Basin Compartments and Seals AAPG Memoir, 61. pp. 153–165.

Banner, J.L., 1995. Application of the trace element and isotope geochemistry of strontium to studies of carbonate diagenesis. *Sediment* **42**, 805–824.

Bishop, P.K., Smalley, P.C., Emery, D., Dickson, J.A.D., 1994. Strontium isotopes as indicators of the dissolving phase in a carbonate aquifer; implications for ^{14}C dating of groundwater. *J. Hydrol.* **154**, 301–321.

Blum, J.D., Gazis, C.A., Jacobson, A.D., Chamberlain, C.P., 1998. Carbonate versus silicate weathering in the Raikhot watershed within the High Himalayan Crystalline Series. *Geology* **26**, 411–414.

Bond, D. C. 1972. In: Hydrodynamics in deep aquifers of the Illinois basin. Illinois State Geological Survey.

Breemer, C.W., Clark, P.U., Haggerty, R., 2002. Modeling the subglacial hydrology of the late Pleistocene Lake Michigan Lobe, Laurentide Ice Sheet. *Geol. Soc. Am. Bull.* **114** (6), 665–674.

Budai, J.M., Martini, A.M., Walter, L.M., Ku, T.C.W., 2002. Fracture-fill calcite as a record of microbial methanogenesis and fluid migration: a case study from the Devonian Antrim Shale, Michigan Basin. *Geofluids* **2**, 163–183.

Burke, W.H., Denison, R.E., Hetherington, E.A., Koepnick, R.B., Nelson, H.F., Otto, J.B., 1982. Variation of seawater $^{87}Sr/^{86}Sr$ throughout Phanerozoic time. *Geology* **10**, 516–519.

Castro, M.C., Stute, M., Schlosser, P., 2000. Comparison of ^{4}He ages and ^{14}C ages in simple aquifer systems: implications for groundwater flow and chronologies. *Appl. Geochem.* **15**, 1137–1167.

Clark, I.D., Fritz, P., 1997. *Environmental Isotopes in Hydrogeology*. Lewis Publishers, New York.

Claypool, G.E., Holser, W.T., Kaplan, I.R., Sakai, H., Zak, I., 1980. The age curves of sulfur and oxygen isotopes in marine sulfate and their mutual interpretation. *Chem. Geol.* **28**, 199–260.

Clayton, R.N., Friedman, I., Graf, D.L., Mayeda, T.K., Meents, W.F., Shimp, N.F., 1966. The origin of saline formation waters. 1. Isotopic composition. *J. Geophys. Res.* **71** (16), 3869–3882.

Collinson, C., Sargent, M.L., Jennings, J.R., 1988. Illinois Basin region. In: Sloss, L.L. (Ed.), *The Geology of North America: Sedimentary Cover—North American Craton: US*, Vol. D-2. The Geological Society of America, pp. 383–426.

Coplen, T. B., Kendall, C. 2000. In: Stable hydrogen and oxygen isotope ratios for selected sites of the US Geological Survey's NASQAN and Benchmark Surface-Water Networks. US Geological Survey. pp. 128–131.

Craig, H., 1961. Isotopic variations in meteoric waters. *Science* **133**, 1702–1703.

Das, N., Horita, J., Holland, H.D., 1990. Chemistry of fluid inclusions in halite from the Salina Group of the Michigan Basin: implications for Late Silurian seawater and the origin of sedimentary brines. *Geochim. Cosmochim. Acta* **54**, 319–327.

Desaulniers, D.E., Cherry, J.A., Fritz, P., 1981. Origin, age and movement of pore water in argillaceous quaternary deposits at four sites in southwestern Ontario. *J. Hydrol.* **50**, 231–257.

Dettman, D.L., Smith, A.J., Rea, D.K., Moore Jr., T.C., Lohmann, K.C, 1995. Glacial meltwater in Lake Huron during early postglacial time as inferred from single-valve analysis of oxygen isotopes in ostracodes. *Quaternary Res.* **43**, 297–310.

Dogramaci, S.S., Herczeg, A.L., Schiff, S.L., Bone, Y., 2001. Controls on ^{34}S and ^{18}O of dissolved sulfate in aquifers of the Murray Basin, Australia and their use as indicators of flow processes. *Appl. Geochem.* **16**, 475–488.

Dorr Jr., J.A., Eschman, D.F., 1970. *Geology of Michigan*. The University of Michigan Press.

Drimmie, R. J., Heemskerk, A. R., Johnson, J. C. 1993. Tritium Analysis. Technical Procedure 1.0, Rev03, p. 28. Environmental Isotope Laboratory, Department of Earth Science, University of Waterloo.

Dutton, A., Wilkinson, B.H., Welker, J.M., Bowen, G.J., Lohmann, K.C., 2005. Spatial distribution and seasonal variation in $^{18}O/^{16}O$ of modern precipitation and river water across the conterminous United States. *Hydrol. Process.* **19**, 4121–4146.

Eberts, S. M., George, L. L. 2000. Regional ground-water flow and geochemistry in the midwestern basins and arches aquifer system in parts of Indiana, Ohio, Michigan, and Illinois. In: Regional Aquifer-System Analysis—Midwestern Basins and Arches. US Geological Survey Professional Paper 1423-C. pp. C1-C103.

Elliot, T., Andrews, J.N., Edmunds, W.M., 1999. Hydrochemical trends, palaeorecharge and groundwater ages in the fissured Chalk aquifer of the London and Berkshire Basins UK. *Appl. Geochem.* **14**, 333–363.

Fontes, J.-C., Garnier, J.-M., 1979. Determination of the initial ^{14}C activity of the total dissolved carbon: a review of the existing models and a new approach. *Water Resour. Res.* **15** (2), 399–413.

Geyh, M.A., Kuenzl, R., 1981. Methane in groundwater and its effect on ^{14}C ground water dating. *J. Hydrol.* **52**, 355–358.

Gieskes, J.M., Rogers, W.C., 1973. Alkalinity determinations in interstitial waters of marine sediments. *J. Sediment. Petrol.* **43**, 272–277.

Gilkeson, R.H., Perry Jr., E.C., Cartwright, K., 1981. Isotopic and geologic studies to identify the sources of sulfate in groundwater containing high barium concentrations. Illinois Department of Energy and Natural Resources. *State Geological Survey Division*, 1–39.

Ging, P. B., Long, D. T., Lee, R. W. 1996. In: Selected geochemical characteristics of ground water from the Marshall aquifer in the central lower peninsula of Michigan. US Geological Survey. p. 19.

Hendry, M.J., Wassenaar, L.I., 2000. Controls on the distribution of major ions in pore waters of a thick surficial aquitard. *Water Resour. Res.* **36** (2), 503–513.

Hoaglund III, J.R., Kolak, J.J., Long, D.T., Larson, G.J., 2004. Analysis of modern and Pleistocene hydrologic exchange between Saginaw Bay (Lake Huron) and the Saginaw Lowlands area. *Geol. Soc. Am. Bull.* **116** (1/2), 3–15.

Hogan, J.F., Blum, J.D., Siegel, D.I., Glaser, P.H., 2000. $^{87}Sr/^{86}Sr$ as a tracer of groundwater discharge and precipitation recharge in the Glacial Lake Agassiz Peatlands, Northern Minnesota. *Water Resour. Res.* **36** (12), 3701–3710.

Husain, M.M., Cherry, J.A., Frape, S.K., 2004. The persistence of a large stagnation zone in a developed regional aquifer, Southwestern Ontario. *Can. Geotech. J.* **41**, 943–958.

Hyeong, K., Capuano, R.M., 2001. Ca/Mg of brines in Miocene/Oligocene clastic sediments of the Texas Gulf Coast: Buffering by calcite/disordered dolomite equilibria. *Geochim. Cosmochim. Acta* **65** (18), 3065–3080.

IAEA/WMO (2001). Global network for isotopes in precipitation. The GNIP database, http://isohis.iaea.org.

Jacobson, A.D., Wasserburg, G.J., 2005. Anhydrite and the Sr isotope evolution of groundwater in a carbonate aquifer. *Chem. Geol.* **214**, 331–350.

Johnson, T.M., DePalo, D.J., 1997. Rapid exchange effects on isotope ratios in groundwater systems. 2. Flow investigation using Sr isotope ratios. *Water Resour. Res.* **33** (1), 197–209.

Karim, A., Veizer, J., 2000. Weathering processes in the Indus River basin; implications from riverine carbon, sulfur, oxygen, and strontium isotopes. *Chem. Geol.* **170** (1-4), 153–177.

Keller, S. J. 1983. In: Analyses of Subsurface Brines of Indiana. Indiana Department of Natural Resources, Geological Survey Occasional Paper 41. pp. 1–30.

Kharaka, Y. K., Gunter, W. D., Aggarwal, P. K., Perkins, E. H., DeBraal, J. D. 1988 In: SOLMINEQ.88: A computer program for geochemical modeling of water–rock interactions. US Geological Survey. pp. 1–207.

Kloppmann, W., Dever, L., Edmunds, W.M., 1998. Residence time of Chalk groundwaters in the Paris Basin and the North German Basin: a geochemical approach. *Appl. Geochem.* **13** (5), 593–606.

Krothe, N.C., Kempton, J.P., 1988. Region 14 central glaciated plains. In: Back, W., Rosenshein, J.S., Seaber, P.R. (Eds.), *Hydrogeology*. The Geological Society of America.

Ku, T. C. W. 2001. Organic carbon–mineral interactions in terrestrial and shallow marine environments. Ph. D. thesis, The University of Michigan.

Ku, T.C.W., Walter, L.M., Coleman, M.L., Blake, R.E., Martini, A.M., 1999. Coupling between sulfur recycling and syndepositional carbonate dissolution: evidence from oxygen and sulfur isotope composition of pore water sulfate, South Florida Platform, USA. *Geochim. Cosmochim. Acta* **63** (17), 2529–2546.

Lloyd, O. B., Lyke, W. L. 1995. In: Ground water atlas of the United States, segment 10-Illinois, Kentucky, Ohio, Tennessee. US Geological Survey.

Long, D.T., Wilson, T.P., Takacs, M.J., Rezabek, D.H., 1988. Stable-isotope geochemistry of saline near-surface ground water: East-central Michigan Basin. *Geol. Soc. Am. Bull.* **100**, 1568–1577.

Lyons, W. B., Churchill, S. E., Carey, A. E. 2002. Paleogroundwater in Northwestern Ohio and the significance of Pleistocene recharge and paleolake sediments. In: 51st Annual Meeting, Geological Society of America, Southeastern Section, 36th Annual Meeting, Geological Society of America, North-Central Section, 43.

Lyons, W.B., Tyler, S.W., Gaudette, H.E., Long, D.T., 1995. The use of strontium isotopes in determining groundwater mixing and brine fingering in a playa spring zone, Lake Tyrrell, Australia. *J. Hydrol.* **167**, 225–239.

Ma, L., Castro, M.C., Hall, C.M., 2004. A Late Pleistocene–Holocene noble gas paleotemperature record in southern Michigan. *Geophys. Res. Lett.* **31**, L23204.

Martini, A.M., Walter, L.M., Budai, J.M., Ku, T.C.W., Kaiser, C.J., Schoell, M., 1998. Genetic and temporal relations between formation waters and biogenic methane: Upper Devonian Antrim Shale, Michigan Basin, USA. *Geochim. Cosmochim. Acta* **62** (10), 1699–1720.

McGillen, M.R., Fairchild, I.J., 2005. An experimental study of incongruent dissolution of $CaCO_3$ under analogue glacial conditions. *J. Glaciol.* **51**, 383–390.

McIntosh, J.C., Walter, L.M., 2005. Volumetrically significant recharge of Pleistocene glacial meltwaters into epicratonic basins: constraints imposed by solute mass balances. *Chem. Geol.* **222**, 292–309.

McIntosh, J.C., Walter, L.M., Martini, A.M., 2002. Pleistocene recharge to midcontinent basins: effects on salinity structure and microbial gas generation. *Geochim. Cosmochim. Acta* **66** (10), 1681–1700.

McIntosh, J.C., Walter, L.M., Martini, A.M., 2004. Extensive microbial modification of formation water geochemistry: Case study from a Midcontinent sedimentary basin, United States. *Geol. Soc. Am. Bull.* **116** (5/6), 743–759.

McNutt, R.H., Frape, S.K., Dollar, P., 1987. A strontium, oxygen and hydrogen isotopic composition of brines, Michigan and Appalachian Basins, Ontario and Michigan. *Appl. Geochem.* **2**, 495–505.

Meents W. F., Bell A. H., Rees O. W., Tilbury W. G. 1952. In: Illinois oil-field brines: their geologic occurrence and chemical composition. Illinois State Geological Survey. pp. 5–38.

Meissner B. D., Long D. T., Lee R. W. 1996. In: Selected geochemical characteristics of ground water from the Saginaw aquifer in the central lower peninsula of Michigan. US Geological Survey. p. 19.

Musgrove, M., Banner, J.L., 2004. Controls on the spatial and temporal variability of vadose dripwater geochemistry: Edwards Aquifer, Central Texas. *Geochim. Cosmochim. Acta* **68** (5), 1007–1020.

Nicholas J. R., Rowe G. L., Brannen J. R. 1996. In: Hydrology, water quality, and effects on drought in Monroe County, Michigan. US Geological Survey. pp. 1–169.

Olcott P. G. 1992. Ground water atlas of the United States: segment 9-Iowa, Michigan, Minnesota, Wisconsin. In: Hydrologic Investigations Atlas. US Geological Survey.

Pearson, F.J., Hanshaw, B.B., 1970. Sources of dissolved carbonate species in groundwater and their effects on carbon-14 dating. In: *Isotope Hydrology*. IAEA, Vienna, pp. 271–286.

Plummer, L.N., Busby, J.F., Lee, R.W., Hanshaw, B.B., 1990. Geochemical modeling of the Madison aquifer in parts of Montana, Wyoming, and South Dakota. *Water Resour. Res.* **26** (9), 1981–2014.

Plummer, L. N., Prestemon, E. C., Parkhurst, D. L., 1994. An interactive code (NETPATH) for modeling NET geochemical reactions along a flow PATH, version 2.0. In: US Geological Survey Water Resources Investigations Report 91-4078. p. 227.

Shaver R. H., Burger A. M., Gates G. R., Gray H. H., Hutchison H. C., Keller S. J., Patton J. B., Rexroad C. B., Smith N. M., Wayne W. J., and Wier C. E. 1970. In: Compendium of Rock-Unit Stratigraphy in Indiana. Indiana Department of Natural Resources, Geological Survey. pp. 1–229.

Sidle, W.C., 2002. $^{18}O_{SO_4}$ and $^{18}O_{H_2O}$ as prospective indicators of elevated arsenic in the Goose River ground-watershed, Maine. *Environ. Geol.* **42**, 350–359.

Siegel, D. I. 1989. Geochemistry of the Cambrian-Ordovician aquifer system in the northern Midwest, United States. In: Regional Aquifer-System Analysis—Northern Midwest Aquifer System. US Geological Survey. pp. D1–D76.

Siegel, D.I., 1990. Sulfur isotope evidence for regional recharge of saline water during continental-glaciation, North-central United States. *Geology* **18** (11), 1054–1056.

Siegel, D.I., 1991. Evidence for dilution of deep, confined ground water by vertical recharge of isotopically heavy Pleistocene water. *Geology* **19** (5), 433–436.

Siegel, D.I., Mandle, R.J., 1984. Isotopic evidence for glacial meltwater recharge to the Cambrian Ordovician aquifer, north-central United States. *Quaternary Res.* **22** (3), 328–335.

Socki, R.A., Karlsson, H.R., Everett, G.K.J., 1992. Extraction technique for the determination of oxygen-18 in water using pre-evacuation glass vials. *Anal. Chem.* **64**, 829–831.

Stueber, A.M., Pushkar, P., Hetherington, E.A., 1987. A strontium isotopic study of formation waters from the Illinois Basin, USA. *Appl. Geochem.* **2**, 477–494.

Stueber, A.M., Walter, L.M., 1991. Origin and chemical evolution of formation waters from Silurian-Devonian strata in the Illinois Basin, USA. *Geochim. Cosmochim. Acta* **55** (1), 309–325.

Stueber, A.M., Walter, L.M., 1994. Glacial recharge and paleohydrologic flow systems in the Illinois Basin—evidence from chemistry of Ordovician carbonate (Galena) formation waters. *Geol. Soc. Am. Bull.* **106** (11), 1430–1439.

Szramek, K., Walter, L.M., 2004. Impact of carbonate precipitation on riverine inorganic carbon mass transport from a mid-continent, forested watershed. *Aquat. Geochem.* **10** (1–2), 99–137.

Szramek, K., Walter, L.M., McCall, P., 2004. Arsenic mobility in groundwater/surface water systems in carbonate-rich Pleistocene glacial drift aquifers (Michigan). *Appl. Geochem.* **19** (7), 1137–1155.

Tamers, M.A., 1975. The validity of radiocarbon dates on groundwater. *Geophys. Surv.* **2**, 217–239.

Taylor C. B. 1977. Tritium enrichment of environmental waters by electrolysis: development of cathodes exhibiting high isotopic separation and precise measurement of tritium enrichment factors. In: International Conference of Low-Radioactivity Measurements and Applications. pp. 131–140.

Veizer, J., Ala, D., Azmy, K., Bruckschen, P., Buhl, D., Bruhn, F., Carden, G.A.F., Diener, A., Ebneth, S., Godderis, Y., Jasper, T., Korte, C., Pawellek, F., Podlaha, O.G., Strauss, H., 1999. $^{87}Sr/^{86}Sr$, $\delta^{13}C$ and $\delta^{18}O$ evolution of Phanerozoic seawater. *Chem. Geol.* **161**, 59–88.

Venneman, T.W., O'Neil, J.R., 1993. A simple and inexpensive method of hydrogen isotope and water analyses of minerals and rocks based on zinc reagent. *Chem. Geol.* **103**, 227–234.

Vugrinovich, R., 1988. Relationships between regional hydrogeology and hydrocarbon occurrences in Michigan, USA. *J. Petrol. Geol.* **11** (4), 429–442.

Weaver, T.R., Frape, S.K., Cherry, J.A., 1995. Recent cross-formational fluid flow and mixing in the shallow Michigan Basin. *Geol. Soc. Am. Bull.* **107** (6), 697–707.

Williams, E. 2005. Carbon cycling and mineral weathering in temperate forested watersheds: an integrated study of solution and soil chemistries. Ph. D. thesis, University of Michigan.

Wilson, T.P., Long, D.T., 1993a. Geochemistry and isotope chemistry of Ca–Na–Cl brines in Silurian strata, Michigan Basin, USA. *Appl. Geochem.* **8**, 507–524.

Wilson, T.P., Long, D.T., 1993b. Geochemistry and isotope chemistry of Michigan Basin brines: Devonian formations. *Appl. Geochem.* **8**, 81–100.

Yu G. H. and Krothe N. C. (1997) Annual variation of $\delta^{13}C$ infiltrating water through a soil profile in a mantled karst area in southern Indiana. In: 30th International Geological Congress. pp. 281–290.